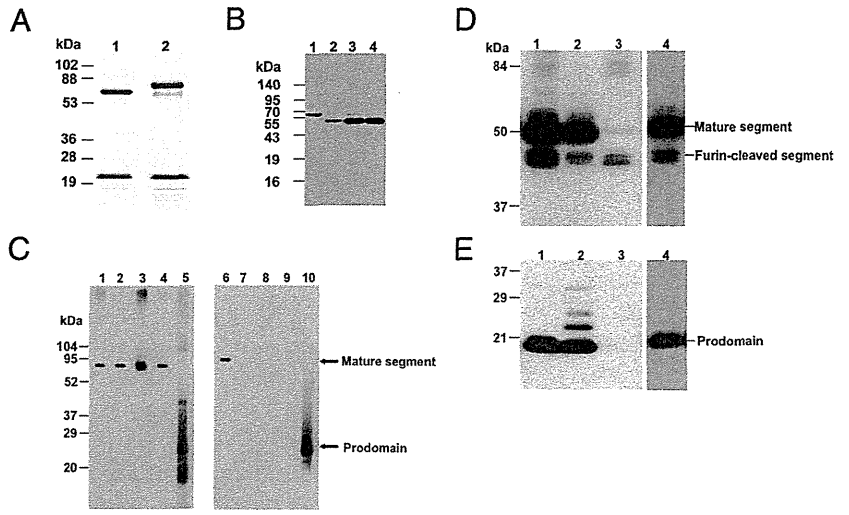

Figure 1. Characterization of recombinant PCSK9 and monoclonal antibodies to PCSK9. (A) Purified rhPCSK9 (0.75 μg) was analyzed by 5–20% SDS-PAGE under nonreducing (lane 1) and reducing (lane 2) conditions and visualized by silver staining. (B) Purified rhPCSK9 (1 μg) digested without (lane 1) or with (lane 2) recombinat furin (0.5 μg) and cell lysate of rhΔ218PCSK9 (lanes 3 and 4) was subjected to SDS-PAGE followed by immunoblotting and detection with anti-Tetra-His antibody. (C) The reactivity of each monoclonal antibody (MAb) to purified rhPCSK9 (1.0 μg) was analyzed by 5–20% SDS-PAGE under nonreducing (lanes 1–5) and reducing (lanes 6–10) condition, followed by immunoblotting as described in the Materials and Methods. Lanes 1 and 6, monoclonal PCSK9 antibody (MAB38881; R&D Systems); lanes 2 and 7, Mab 1FB; lanes 3 and 8, Mab B12E; lanes 4 and 9, Mab B1G; lanes 5 and 10, Mab G12D. (D) The immunoprecipitation of human plasma with Mabs against PCSK9 was carried out. Immunoprecipitates were separated by a 5–20% SDS-PAGE under nonreducing condition, followed by immunoblotting and detection with monoclonal PCSK9 antibody (MAB38881). Lane 1, Mab 1FB; lane 2, Mab G12D; lane 3, Mab B1G; lane 4, Mab B12E. (E) The immunoprecipitation of human plasma with Mabs against PCSK9 was carried out. Immunoprecipitates were separated by a 5–20% SDS-PAGE under a nonreducing condition, followed by immunoblotting and detection with Mab G12D. Lane 1, Mab 1FB; lane 2, Mab G12D; lane 3, Mab B1G; lane 4, Mab B12E.

plasma TC, LDL-C, TG, ApoB, ApoC-II, ApoC-III, ApoE, and Lp(a), while the plasma levels of HDL-C, ApoA-I, and ApoA-II decreased by 13–16% (Table 1 and Supplemental Table 2). In FH heterozygotes, a similar reduction was shown.

Removal of PCSK9s in FH homozygotes or heterozygotes by LDL-A with DS columns

In FH homozygotes, the plasma levels of mature and furin-cleaved PCSK9 averaged 490 ± 173 ng/mL and 74 ± 23 ng/mL, respectively, before LDL-A treatment. The two forms of PCSK9 were, respectively, reduced by 56% and 55% in FH homozygotes by a single LDL-A procedure (Figure 2A). Furin-cleaved PCSK9 constituted approximately 15% of circulating PCSK9 in the plasma of FH patients. In FH heterozygotes, the plasma levels of the two forms of PCSK9 averaged 443 ± 128 ng/mL and 55 ± 26 ng/mL, respectively, before LDL-A treatment. The two forms of PCSK9 were reduced by 46% and 48% by a single LDL-A procedure in FH heterozygotes (Figure 2B). Thus, there were no significant differences in the reduction rate of either form of plasma PCSK9 after LDL-A between FH homozygotes and heterozygotes. In addition, plasma levels of both PCSK9s in FH homozygotes before LDL-A treatment were not significantly different from those in the plasma of FH heterozygotes. As shown in Figure 3, there was a high degree of correlation between the reduction of plasma LDL-C and the reduction of mature PCSK9 in both FH homozygotes ($r = 0.79$; $P = .036$) and heterozygotes ($r = 0.79$; $P = .004$). In addition, there was a significant correlation between the reduction in plasma Lp(a) and that in mature PCSK9 in FH heterozygotes ($r = 0.74$; $P = .0098$; data not shown). On the other hand, there was no correlation between the reductions in plasma HDL-C and mature PCSK9 in FH homozygotes or heterozygotes (Supplemental Figure 4).

Crossover study of LDL-A treatment with DM columns in FH heterozygotes

A crossover study comparing the treatment efficacy between DS and DM columns was performed in 5 FH heterozygotes. A single LDL-A treatment with DM columns produced a 49–68% reduction in plasma TC, LDL-C, TG, ApoB, ApoC-II, ApoC-III, ApoE, and Lp(a), while the plasma levels of HDL-C, ApoA-I, and ApoA-II decreased by 23–26% (Supplemental Table 3). The plasma levels of mature and furin-cleaved PCSK9 before LDL-A treatment averaged 282 ± 36 ng/mL and 43 ± 28 ng/mL, respectively; the two forms were decreased by 56% and 48% by a single LDL-A treatment (Figure 2C).

Gel filtration chromatography of PCSK9 before and after a single LDL-A treatment

The plasma obtained before and after the single LDL-A treatment with DS columns was separated by gel filtration chromatography, and cholesterol and both forms of PCSK9 were measured in each fraction. Typical distribution patterns of cholesterol and PCSK9s are shown in Figure 4. Cholesterol levels were markedly reduced in the LDL fraction, while there was little change in the HDL fraction. Approximately 20% of mature PCSK9 coeluted with the apoB-containing fraction, and the rest coeluted with the apoB-deficient fraction. Meanwhile, in a portion of the FH patients, less than 5% of total PCSK9 was ob-

Table 1. Laboratory Data in FH Homozygotes and Heterozygotes Before and After a Single LDL-A Treatment With DS Columns

	FH homozygotes (n = 7)			FH heterozygotes (n = 11)		
(mg/dL)	Before	After	Reduction (%)	Before	After	Reduction (%)
TC	288 ± 63	86 ± 24[a]	70	220 ± 77	89 ± 41[a]	59
LDL-C	237 ± 49[d]	55 ± 22[a]	76	164 ± 75	51 ± 33[a]	69
HDL-C	31 ± 12	26 ± 9[a]	16	36 ± 18	32 ± 16	13
TG	99 ± 60	27 ± 21[a]	74	97 ± 43	30 ± 22[a]	70
Apo A-I	81 ± 22	71 ± 20[a]	13	99 ± 39	88 ± 35[a]	11
Apo A-II	22 ± 4	18 ± 4[a]	15	25 ± 8	21 ± 7[a]	14
Apo B	182 ± 44[d]	40 ± 21[a]	78	124 ± 46	36 ± 23[a]	71
Apo C-II	3.0 ± 2.3	1.3 ± 0.8[b]	54	3.6 ± 1.8	1.8 ± 1.3[a]	54
Apo C-III	8.5 ± 4.5	3.5 ± 1.6[a]	57	8.5 ± 2.8	4.6 ± 2.4[a]	48
Apo E	6.5 ± 2.1[c]	1.5 ± 0.8[a]	76	4.1 ± 0.8	1.1 ± 0.5[a]	73
Lp(a)	27 ± 22[d]	8.1 ± 5.8[b]	67	55 ± 27	19 ± 16[a]	68

Abbreviations: FH, familial hypercholesterolemia; HDL-C, high-density lipoprotein-cholesterol; LDL-C, low-density lipoprotein-cholesterol; Lp(a), lipoprotein (a); TC, total cholesterol; TG, triglyceride. All values are shown as mean ± SD.

n = 6 in Lp(a) of FH homozygotes.

[a] $P < 0.01$.

[b] $P < 0.05$ vs the respective values before LDL-A.

[c] $P < 0.01$.

[d] $P < 0.05$ vs the respective values in FH heterozygotes.

served in the apoB-fraction (data not shown). The distribution pattern of furin-cleaved PCSK9 was similar to that of mature PCSK9. Both forms of PCSK9s in the apoB-deficient fraction were reduced by 52–54%, while those in the apoB-containing fraction were reduced by 92–97%.

Coimmunoprecipitation of apoB in plasma of FH

To examine the association of apoB with PCSK9, plasma samples of FH were immunoprecipitated with monoclonal anti-apoB antibody. The control samples that were incubated in nonimmune serum instead of apoB antibody and negative control samples that were incubated in only resin showed no bands reactive to anti-apoB antibody (Figure 5A). Based on the coimmunoprecipitates of apoB, a mature PCSK9 band was detected by polyclonal PCSK9 antibody, confirming an association between mature PCSK9 and apoB in the plasma of FH. The band of furin-cleaved PCSK9 could not be detected in coimmunoprecipitation of apoB, because it overlapped that of IgG (data not shown).

Profile of Lp(a) by gel filtration chromatography

To examine the association of Lp(a) with PCSK9 in the plasma of FH, Lp(a) was measured by ELISA in the collected fractions obtained by gel filtration analysis. Lp(a) was recovered predominantly in apoB-containing fraction, and was not recovered in the apoB-deficient fraction which contains the highest levels of both PCSK9s (Figure 5B).

Discussion

In the present study, we demonstrated that the two forms of plasma PCSK9 were removed by LDL-A treatment with either DS or DM columns in both FH homozygotes and heterozygotes based on measurements using a new sandwich ELISA. The two forms of PCSK9 were significantly decreased by 55–56% in FH homozygotes after a single LDL-A treatment with DS columns, and were decreased to a similar extent in FH heterozygotes after the treatment with DS or DM columns. The removal of two forms of PCSK9 would have contributed to some extent to the control of LDL-C medi-

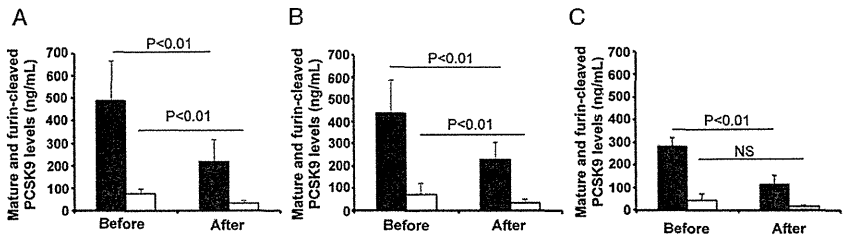

Figure 2. Change of plasma mature and furin-cleaved PCSK9 levels before and after a single LDL-A treatment. Plasma levels of mature (closed column) and furin-cleaved (open column) PCSK9s in (A) FH homozygotes (N = 7), (B) FH heterozygotes (N = 11) before and after LDL-A treatment with DS columns, and in (C) FH heterozygotes (N = 5) before and after LDL-A treatment with DM columns are shown.

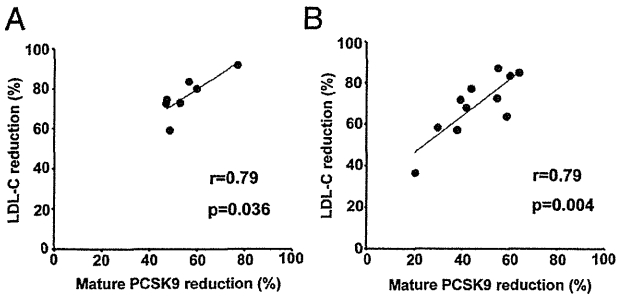

Figure 3. Correlation between plasma LDL-C reduction and mature PCSK9 reduction in FH homozygotes and FH heterozygotes. (A) Correlation between plasma LDL-C reduction (Y-axis) and mature PCSK9 reduction (X-axis) in FH homozygotes after a single LDL-A treatment with DS columns (N = 7). (B) Correlation between plasma LDL-C reduction (Y-axis) and mature PCSK9 reduction (X-axis) in FH heterozygotes after a single LDL-A treatment with DS columns (N = 11).

ated by LDLR in heterozygous FH or receptor-defective homozygous FH patients undergoing LDL-A treatment. However, it would not have contributed to the control of LDL-C in receptor-negative homozygous FH patients. In addition, DM columns whose treated volumes are limited are not usually used for patients who need a high volume of treated plasma. The use of DS columns is contraindicated for patients taking angiotensin-converting enzyme (ACE) inhibitors. Thus, we cannot decide whether DS or DM columns are superior, but we need to decide an appropriate application for each case.

Statins, the most effective commercially available medication for lowering serum LDL-C, decrease cholesterol synthesis, and increase LDLR activity in the liver. Meanwhile, they also stimulate expression of PCSK9, thereby reducing their own effects (23, 24). Thus, antisense oligonucleotides, RNA-mediated interference and Mabs that target PCSK9 have been developed as new treatment strategies for lowering LDL-C (25–29). The use of PCSK9-MAb could reduce the frequency of LDL-A and control LDL-C in heterozygous FH or homozygous FH patients with the LDLR defective type. In addition, the combination of PCSK-Mab and LDL-A treatment may improve the control of LDL-C synergistically or additively.

Recently, Dubic et al has developed an ELISA for the measurement of total PCSK9 using polyclonal antibodies (5). In the present study, we developed a new sandwich ELISA using Mabs for plasma mature and furin-cleaved PCSK9s, respectively, for the first time. This ELISA method could clarify association of the ratio of each form of PCSK9 with the effects of medication in hyperlipidemia patients with gain- or loss-of-function PCSK9 mutations and those taking cholesterol-lowering drugs (30), and with various conditions of hyperlipidemia concomitant with type II diabetes, obesity, and so on. In addition, it has been reported that furin-cleaved PCSK9 represents up to 40% of the total PCSK9 in normal subjects (9), whereas it

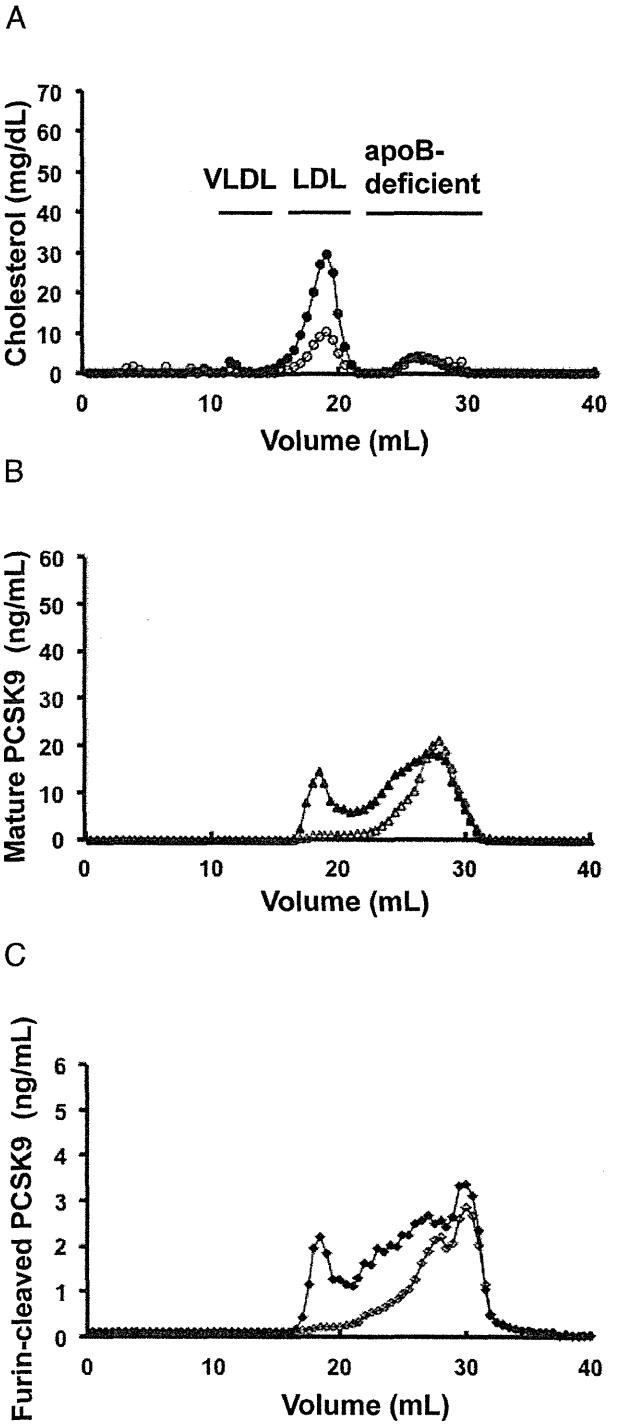

Figure 4. Typical gel filtration chromatography of mature and furin-cleaved PCSK9s and cholesterol in FH plasma before and after LDL-A treatment. Profiles of cholesterol (A, closed circles: before; open circles: after), mature (B, closed triangles: before; open triangles: after), and furin-cleaved PCSK9s (C, closed diamonds: before; open diamonds: after) were analyzed in FH plasma before and after a single LDL-A treatment with DS columns after fractionation by gel filtration chromatography as described in Materials and Methods.

represented 15% of the total PCSK9 in FH patients in the present study. We thus formed a hypothesis that FH shows high LDL-C levels due to not only LDLR mutations but also higher activity of LDLR degradation. The association

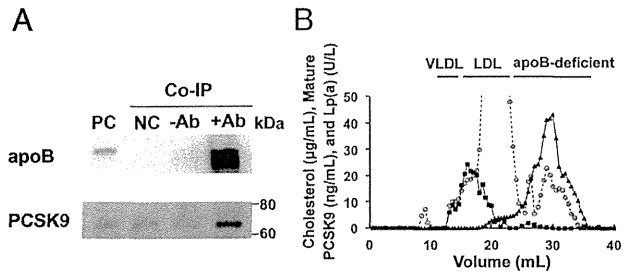

Figure 5. Coimmunoprecipitation of apoB and profile of Lp(a) by gel filtration chromatography in FH plasma. (A) Immunoprecipitation (IP) was performed with 500 μL of plasma from an FH patient treated by 1% triton X-100 and 0.5% sodium deoxycholate (final concentration). An equal volume of supernatants was also applied to columns without IgG and processed in the same way as the antibody coupling resin [negative control (NC)]. The immunoprecipitates were separated by 8–16% SDS-PAGE under denaturing and reducing conditions followed by immunoblotting with monoclonal anti-apoB antibody or polyclonal anti-PCSK9 antibody, and mouse TrueBlot® ULTRA: Anti-Mouse Ig HRP (eBioscience) or HRP-linked anti sheep IgG antibody (Santa Cruz Biotechnology Inc.). Control samples that were incubated in nonimmune serum were also analyzed (-Ab). The bands of apoB and PCSK9 were examined in an apoB-IP sample (+Ab). PC; positive control, -Ab; control-IP, +Ab; apoB-IP. (B) Profiles of Lp(a), cholesterol, and mature PCSK9 levels in the plasma from an FH patient as determined by gel filtration chromatography. Their levels in the collected fractions were measured as described in Materials and Methods. Closed squares: Lp(a); open circles: cholesterol; closed triangles: mature PCSK9 in plasma before LDL-A.

of the ratio of each form of PCSK9 with the regulation of LDL-C metabolism would be validated by the present method.

Gel filtration chromatography analysis showed that 20% of the total plasma PCSK9s existed in the apoB-containing fraction, which is a typical profile for plasma PCSK9 in FH patients (Figure 4). It has previously been reported that 35–39% or > 40% of PCSK9 was associated with the LDL fraction in normolipidemic subjects by size exclusion chromatography or natural density gradient (31, 32). Thus, it was suggested that the amount of PCSK9 contained in the apoB-containing fraction in the plasma of FH patients was lower than that in normolipidemic subjects. Two forms of PCSK9 were reduced by 92–97% in the LDL fraction on gel filtration chromatography and the reduction in mature PCSK9 was strongly correlated with that in LDL-C after a single LDL-A treatment (Figure 3). By immunoprecipitation, plasma mature PCSK9 was confirmed to be bound to apoB (Figure 5A). Thus, it was suggested that a portion of plasma PCSK9 was removed in association with apoB by LDL-A. The distribution of Lp(a) was not overlapped like that of mature PCSK9, suggesting that mature PCSK9 was not associated with Lp(a) (Figure 5B). In addition, the reason why PCSK9 associated with LDL decreases more than LDL-C has not been clarified. Further studies are necessary to clarify the mechanism underlying the removal of the proportion of PCSK9 associated with LDL by LDL-A.

Recently, it has been reported that LDL-bound PCSK9 in human plasma exhibits diminished binding activity toward cell surface LDLR (31). However, it has not been clarified whether PCSK9-associated LDL is incorporated by LDLR, and further studies will be needed to examine the question. In addition, the interaction between apoB and PCSK9 has been reported to inhibit intracellular degradation of apoB and to result in increased secretion of apoB-containing lipoproteins (33). This secreted PCSK9-associated apoB may be derived from LDL associated with PCSK9 in plasma. A portion of PCSK9 may be bound to LDL extracellularly, thereby promoting cellular degradation of LDLR in the endosome.

In the present study, we found that the two forms of PCSK9 were reduced by 52–54% in the apoB-deficient fraction from gel filtration chromatography analysis. Circulating mature and furin-cleaved PCSK9s were mainly present in the apoB-deficient fraction. PCSK9s were removed by apoB-independent pathways based on the electric charge or nonspecific binding to the DS columns while they were removed based on particle size or nonspecific binding to the DM columns. The apoB-deficient fraction has been reported to contain PCSK9 that is mostly of a higher molecular weight, likely dimers and trimers (16, 32, 34). In addition, a previous study has shown that various proteins are present in this fraction, including albumin, globulin, serum amyloid-A, and more (35). LDL-A is thus suggested to remove circulating PCSK9 that is of high molecular weight, likely a dimmer or trimer, in association with these proteins in the apoB-deficient fraction. Meanwhile, other lipoproteins such as HDL have been reported to affect the self-association of PCSK9 (35). It has been calculated that two forms of PCSK9 are negatively charged (mature PCSK9: pI = 6.6; furin-cleaved PCSK9: pI = 7.02) (16), so they are not likely to bind directly to the DS column which is also negatively charged. A future study will be required to investigate the forms of PCSK9 in the apoB-deficient fraction.

The result that PCSK9 was removed by LDL-A in homozygous FH is not consistent with the report by Cameron et al (17). Because the columns used in their study were not described, they may have been different from those used in our present study or the study by Tavori et al (16). Thus, the differences in columns, race, life-style, forms of PCSK9 in plasma and proteins associated with PCSK9 may affect the removal of PCSK9 by LDL-A.

This study has some limitations. The major limitation is that a small sample size of 5 may be insufficient to test subtle differences between the two methods of apheresis on PCSK9. However, we could not get enough subjects for a crossover study comparing the treatment efficacy between DS and DM columns. A second limitation is that we

did not perform a time-dependent study of rebound trajectories in LDL-C, apoB, Lp(a), and PCSK9 in the interval between apheresis. That could provide greater insight into the mechanisms of the coordinated regulation of apoB, Lp(a), and PCSK9. A third limitation is that the number of gel filtration analyses was limited because there were not enough plasma residues for analysis.

In conclusion, our present study has shown that plasma mature and furin-cleaved PCSK9s were removed in FH homozygotes and heterozygotes by binding to apoB or other mechanisms. This report is also the first to demonstrate for an ELISA method to measure both forms of plasma PCSK9–mature and furin-cleaved form–and this technique is expected to be useful for investigating the effects of medications or the physiological or pathological roles of PCSK9.

Acknowledgments

We thank Dr. Kazuyuki Ogawa and Mr. Tadao Iwasaki for measurement of the plasma mature and furin-cleaved PCSK9 concentrations, Mr. Koji Ogawa and Mr. Teruyuki Hayashi for sample collection, Ms. Hitomi Komai for experimental support, Dr. Ryo Koezuka for clinical suggestions, and Ms. Chisato Takeuchi for help in the clinical information from Kenporen Osaka Central Hospital.

Address all correspondence and requests for reprints to: Mariko Harada-Shiba, MD, PhD, Department of Molecular Innovation in Lipidology, National Cerebral and Cardiovascular Center Research Institute, 5–7–1 Fujishirodai, Suita, Osaka 565–8565, Japan. E-mail: mshiba@ ncvc.go.jp.

This work was supported by Grants-in-Aid for Scientific Research from the Japanese Ministry of Health, Labor, and Welfare (H23-seisaku tansaku-ippan-004 and H23-nanji-ippan-011) and Intramural Research Fund (25-2-5) for Cardiovascular Diseases of National Cerebral and Cardiovascular Center.

Disclosure Summary: M.H., H.M., K.Y., T.T., and I.K. have nothing to disclose. Y.Y. is a trainee from Kaneka Corporation. M.H-S. received grant support (2013) from Kaneka Corporation and is an inventor of Japan Patent Kokai 2012-237752. M.I., T.K., and H.H. are inventors of Japan Patent Kokai 2012-237752 and are employed by BML, Inc.

References

1. Goldstein JL, Hobbs HH, Brown MS. Familial hypercholesterolemia. In: Scriver CR BA, Sly WS, Valle D, eds. *The Metabolic and Molecular Bases of Inherited Disease.* 8th ed. New York: McGraw-Hill; 2001.
2. Abifadel M, Varret M, Rabès JP, et al. Mutations in PCSK9 cause autosomal dominant hypercholesterolemia. *Nature Genetics.* 2003; 34:154–156.
3. Benjannet S, Rhainds D, Essalmani R, et al. NARC-1/PCSK9 and its natural mutants: zymogen cleavage and effects on the low density lipoprotein (LDL) receptor and LDL cholesterol. *J Biol Chem.* 2004; 279:48865–48875.
4. Maxwell KN, Breslow JL. Adenoviral-mediated expression of Pcsk9 in mice results in a low-density lipoprotein receptor knockout phenotype. *Proc Natl Acad Sci USA.* 2004;101:7100–7105.
5. Dubuc G, Tremblay M, Paré G, et al. A new method for measurement of total plasma PCSK9: clinical applications. *J Lipid Res.* 2010; 51:140–149.
6. Alborn WE, Cao G, Careskey HE, et al. Serum proprotein convertase subtilisin kexin type 9 is correlated directly with serum LDL cholesterol. *Clin Chem.* 2007;53:1814–1819.
7. Benjannet S, Rhainds D, Hamelin J, Nassoury N, Seidah NG. The proprotein convertase (PC) PCSK9 is inactivated by furin and/or PC5/6A: functional consequences of natural mutations and post-translational modifications. *J Biol Chem.* 2006;281:30561–30572.
8. Essalmani R, Susan-Resiga D, Chamberland A, et al. In vivo evidence that furin from hepatocytes inactivates PCSK9. *J Biol Chem.* 2011;286:4257–4263.
9. Han B, Eacho PI, Knierman MD, et al. Isolation and characterization of the circulating truncated form of PCSK9. *J Lipid Res.* 2014; 55:1505–1514.
10. Lipari MT, Li W, Moran P, et al. Furin-cleaved proprotein convertase subtilisin/kexin type 9 (PCSK9) is active and modulates low density lipoprotein receptor and serum cholesterol levels. *J Biol Chem.* 2012;287:43482–43491.
11. Yokoyama S, Hayashi R, Satani M, Yamamoto A. Selective removal of low density lipoprotein by plasmapheresis in familial hypercholesterolemia. *Arteriosclerosis.* 1985;5:613–622.
12. Makino H, Harada-Shiba M. Long-term effect of low-density lipoprotein apheresis in patients with homozygous familial hypercholesterolemia. *Ther Apher Dial.* 2003;7:397–401.
13. Kobayashi J, Katsube S, Shimoda M, et al. Single LDL apheresis improves serum remnant-like particle-cholesterol, C-reactive protein, and malondialdehyde-modified-low-density lipoprotein concentrations in Japanese hypercholesterolemic subjects. *Clin Chim Acta.* 2002;321:107–112.
14. Kojima S, Harada-Shiba M, Toyota Y, et al. Changes in coagulation factors by passage through a dextran sulfate cellulose column during low-density lipoprotein apheresis. *Int J Artif Organs.* 1992;15:185–190.
15. Yuasa Y, Osaki T, Makino H, et al. Proteomic analysis of proteins eliminated by low-density lipoprotein apheresis. *Ther Apher Dial.* 2014;18:93–102.
16. Tavori H, Giunzioni I, Linton MF, Fazio S. Loss of plasma proprotein convertase subtilisin/kexin 9 (PCSK9) after lipoprotein apheresis. *Circ Res.* 2013;113:1290–1295.
17. Cameron J, Bogsrud MP, Tveten K, et al. Serum levels of proprotein convertase subtilisin/kexin type 9 in subjects with familial hypercholesterolemia indicate that proprotein convertase subtilisin/kexin type 9 is cleared from plasma by low-density lipoprotein receptor-independent pathways. *Transl Res.* 2012;160:125–130.
18. Mabuchi H, Miyamoto S, Ueda K, et al. Causes of death in patients with familial hypercholesterolemia. *Atherosclerosis.* 1986;61:1–6.
19. Harada-Shiba M, Arai H, Oikawa S, et al. Guidelines for the management of familial hypercholesterolemia. *J Atheroscler Thromb.* 2012;19:1043–1060.
20. Harada-Shiba M, Takagi A, Miyamoto Y, et al. Clinical features and genetic analysis of autosomal recessive hypercholesterolemia. *J Clin Endocrinol Metab.* 2003;88:2541–2547.
21. Ishihara M, Kujiraoka T, Iwasaki T, et al. A sandwich enzyme-linked immunosorbent assay for human plasma apolipoprotein A-V concentration. *J Lipid Res.* 2005;46:2015–2022.
22. Oka T, Kujiraoka T, Ito M, et al. Distribution of phospholipid transfer protein in human plasma: presence of two forms of phospholipid transfer protein, one catalytically active and the other inactive. *J Lipid Res.* 2000;41:1651–1657.
23. Dubuc G, Chamberland A, Wassef H, et al. Statins upregulate PCSK9, the gene encoding the proprotein convertase neural apop-

tosis-regulated convertase-1 implicated in familial hypercholesterolemia. *Arterioscler Thromb Vasc Biol.* 2004;24:1454–1459.
24. **Dong B, Wu M, Li H, et al.** Strong induction of PCSK9 gene expression through HNF1alpha and SREBP2: mechanism for the resistance to LDL-cholesterol lowering effect of statins in dyslipidemic hamsters. *J Lipid Res.* 2010;51:1486–1495.
25. **Frank-Kamenetsky M, Grefhorst A, Anderson NN, et al.** Therapeutic RNAi targeting PCSK9 acutely lowers plasma cholesterol in rodents and LDL cholesterol in nonhuman primates. *Proc Natl Acad Sci USA.* 2008;105:11915–11920.
26. **Yamamoto T, Harada-Shiba M, Nakatani M, et al.** Cholesterol-lowering action of BNA-based antisense oligonucleotides targeting PCSK9 in atherogenic diet-induced hypercholesterolemic mice. *Mol Therapy Nucleic Acids.* 2012;1:e22.
27. **Chan JC, Piper DE, Cao Q, et al.** A proprotein convertase subtilisin/kexin type 9 neutralizing antibody reduces serum cholesterol in mice and nonhuman primates. *Proc Natl Acad Sci USA.* 2009;106:9820–9825.
28. **Stein EA, Gipe D, Bergeron J, et al.** Effect of a monoclonal antibody to PCSK9, REGN727/SAR236553, to reduce low-density lipoprotein cholesterol in patients with heterozygous familial hypercholesterolaemia on stable statin dose with or without ezetimibe therapy: a phase 2 randomised controlled trial. *Lancet.* 2012;380:29–36.
29. **Giugliano RP, Desai NR, Kohli P, et al.** Efficacy, safety, and tolerability of a monoclonal antibody to proprotein convertase subtilisin/kexin type 9 in combination with a statin in patients with hypercholesterolaemia (LAPLACE-TIMI 57): a randomised, placebo-controlled, dose-ranging, phase 2 study. *Lancet.* 2012;380:2007–2017.
30. **Nozue T, Hattori H, Ishihara M, et al.** Comparison of effects of pitavastatin versus pravastatin on serum proprotein convertase subtilisin/kexin type 9 levels in statin-naïve patients with coronary artery disease. *Am J Cardiol.* 2013;111:1415–1419.
31. **Kosenko T, Golder M, Leblond G, Weng W, Lagace TA.** Low density lipoprotein binds to proprotein convertase subtilisin/kexin type-9 (PCSK9) in human plasma and inhibits PCSK9-mediated low density lipoprotein receptor degradation. *J Biol Chem.* 2013;288:8279–8288.
32. **Tavori H, Fan D, Blakemore JL, et al.** Serum proprotein convertase subtilisin/kexin type 9 and cell surface low-density lipoprotein receptor: evidence for a reciprocal regulation. *Circulation.* 2013;127:2403–2413.
33. **Sun H, Samarghandi A, Zhang N, Yao Z, Xiong M, Teng BB.** Proprotein convertase subtilisin/kexin type 9 interacts with apolipoprotein B and prevents its intracellular degradation, irrespective of the low-density lipoprotein receptor. *Arterioscler Thromb Vasc Biol.* 2012;32:1585–1595.
34. **Fan D, Yancey PG, Qiu S, et al.** Self-association of human PCSK9 correlates with its LDLR-degrading activity. *Biochemistry.* 2008;47:1631–1639.
35. **Holzer M, Trieb M, Konya V, Wadsack C, Heinemann A, Marsche G.** Aging affects high-density lipoprotein composition and function. *Biochim Biophys Acta.* 2013;1831:1442–1448.

NUCLEIC ACID THERAPEUTICS
Volume 24, Number 4, 2014

DOI: 10.1089/nat.2013.0470

Brief Communication

Evaluation of Multiple-Turnover Capability of Locked Nucleic Acid Antisense Oligonucleotides in Cell-Free RNase H-Mediated Antisense Reaction and in Mice

Tsuyoshi Yamamoto,[1] Naoko Fujii,[1] Hidenori Yasuhara,[1] Shunsuke Wada,[1] Fumito Wada,[1] Naoya Shigesada,[1] Mariko Harada-Shiba,[2] and Satoshi Obika[1]

The multiple-turnover ability of a series of locked nucleic acid (LNA)-based antisense oligonucleotides (AONs) in the RNase H-mediated scission reaction was estimated using a newly developed cell-free reaction system. We determined the initial reaction rates of AONs under multiple-turnover conditions and found that among 24 AONs tested, AONs with melting temperatures (*T*m) of 40°C–60°C efficiently elicit multiple rounds of RNA scission. On the other hand, by measuring *T*m with two 10-mer RNAs partially complementary to AONs as models of cleaved 5′ and 3′ fragments of mRNA, we found that AONs require adequate binding affinity for efficient turnover activities. We further demonstrated that the efficacy of a set of 13-mer AONs in mice correlated with their turnover efficiency, indicating that the intracellular situation where AONs function is similar to multiple-turnover conditions. Our methodology and findings may provide an opportunity to shed light on a previously unknown antisense mechanism, leading to further improvement of the activity and safety profiles of AONs.

Introduction

ANTISENSE OLIGONUCLEOTIDES (AONs) having specific configurations compatible with RNase H-inducible capacity have been developed over decades and have been shown to be very powerful and robust gene silencing materials in cultured cells and animals, as well as in humans (Crooke, 2007; Yamamoto et al., 2011). In particular, the "gapmer" configuration, which is a chimeric AON consisting of a central RNase H-recruitable DNA stretch pinched by affinity-enhancing modified nucleic acids with fully phosphorothioated (PS) internucleotide linkages, has shown great promise. Affinity-enhancing modified nucleic acids, such as MOE (2′-*O*-methoxyethyl RNA), 2′,4′-BNA/LNA (2′-*O*,4′-*C*-methylene bridged nucleic acid/locked nucleic acid) (Fig. 1A) (Obika et al., 1997; Obika et al., 1998; Singh et al., 1998), and other bridged nucleic acids (BNAs) (Hari et al., 2006; Miyashita et al., 2007; Seth et al., 2009; Prakash et al., 2010; Yahara et al., 2012) mostly interfere with RNase H activity, but when used in a chimeric gapmer, they assist in enhancing target binding and nuclease stability, greatly improving its potency without affecting RNase H capacity. Despite these innovations, very few products have been released on the market and some candidates in clinical trials have been dropped due to efficacy and safety issues.

More recently, Straarup et al. successfully improved efficacy of an earlier LNA-based gapmer targeting apolipoprotein B-100 (apoB) by trimming its conventional long-strand [16∼20 nucleotides (nt)] and utilizing the resulting shorter LNA gapmers (∼13 nt) (Straarup et al., 2010). Our group also independently reproduced and extended this observation by using newly developed 2′,4′-BNA^{NC} chemistry and supported the unusual notion that a drug with weaker binding has stronger silencing activity (Fig. 1A) (Yamamoto et al., 2012b). One possible explanation for this finding is that shorter AONs accelerate the reaction to a greater degree than conventional AONs *via* turnover mechanisms. Stanton et al. recently observed that melting temperatures (*T*m) of greater than 80°C showed reduced silencing activity and explained this finding as a result of an inability to recycle AONs in cells (Stanton et al., 2012). However, to the best of our knowledge, there is no experimental evidence of AON turnover, despite its anticipated importance as in RNAi mechanisms (Hutvagner and Zamore, 2002). If turnover of AONs was demonstrated in antisense mechanisms, a more favorable configuration or chemistry that accelerates AON turnover may be discovered, and this discovery could lead to additional insights into strategies for further improving the activity and safety of AONs. Most previous works related to antisense reaction kinetics have been conducted to determine whether duplexes of interest have an ability to elicit RNase H, and are thus performed under excess amounts of AON/RNA duplex over RNase H in cell-free systems (single-turnover conditions for AON) (Crooke et al., 1995; Lima and Crooke,

[1]Graduate School of Pharmaceutical Sciences, Osaka University, Suita, Osaka, Japan.
[2]Department of Molecular Innovation in Lipidology, National Cerebral and Cardiovascular Center Research Institute, Suita, Osaka, Japan.

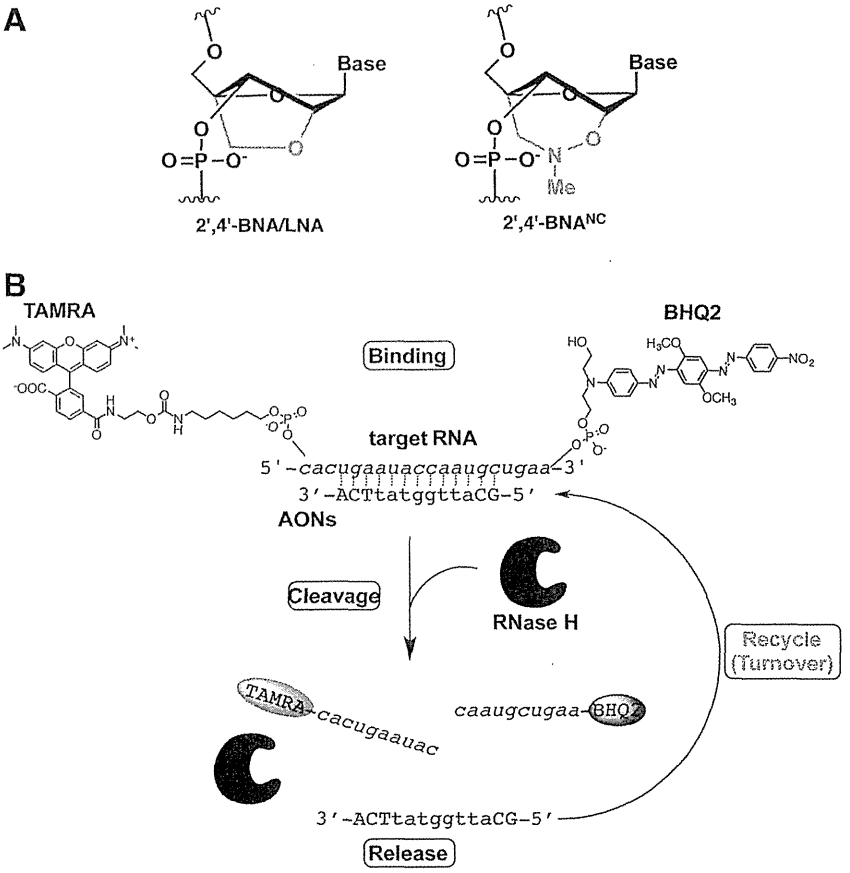

FIG. 1. Recycling of antisense oligonucleotides in antisense reaction. **(A)** Structures of bridged nucleic acids (BNAs). **(B)** Schematic illustration of cell-free Förster resonance energy transfer (FRET)-based turnover monitoring system used in this study. Color images available online at www.liebertpub.com/nat

1997; Vester et al., 2008; Stanton et al., 2012). In the present study, to investigate whether AONs are recyclable in antisense reactions, we devised a cell-free reaction system, in which synthetic 20-mer target RNA conjugated with a pair of FRET (Förster resonance energy transfer) dyes and *E*scherichia *coli*–derived RNase H are both in excess over AONs (multiple-turnover conditions). In this system, an increase in fluorescence from the FRET donor is observed after binding, cleavage, and release proceeds sequentially (Fig. 1B). The main problem facing previous works is the potential difficulty in separating affinity issues from length issues, because affinity usually varies as a function of strand length. In this study, we utilized LNA, which enables us to freely modify AON affinity without changing length; thus, we prepared a series of LNA-based apoB-targeting AONs with a central focus on 13-mer AONs (Table 1), one of which (ApoB-13a) had been previously characterized as highly potent *in vitro* and *in vivo* (Straarup et al., 2010; Yamamoto et al., 2012b).

Materials and Methods

Oligonucleotides

All oligonucleotides listed in Table 1 were purchased from Gene Design Inc.

Thermal denaturation experiments

Thermal denaturation experiments were carried out on SHIMADZU UV-1650 and UV-1800 spectrometers equipped with a *T*m analysis accessory. For duplex formation, equimolecular amounts of target RNA and each AON were dissolved in 10 mM sodium phosphate buffer (pH = 7.2) containing 100 mM (1.0 M for MRNA-1, MRNA-2) NaCl to give a final strand concentration of 2.0 μM. Duplex samples were then annealed by heating at 90°C, followed by slow cooling to room temperature. Melting profiles were recorded at 260 nm from 0°C to 95°C at a scan rate of 0.5°C/minute. Melting temperatures were obtained as maxima of the first derivative of the melting curves.

Turnover experiments

Dual-labeled complementary RNA probe (DL-MRNA) and non-labeled complementary 20-mer RNA (NL-MRNA) were combined in a 1:3 molar ratio. The intended amounts of the resulting mixture and AON were added to RNase H reaction buffer (New England Biolabs). The reaction was initiated by addition of 1 μL of the intended concentrations of *E. coli* RNase H (Takara) to 199 μL of reaction mixture. Fluorescence intensity was recorded once every 15 seconds for 15 minutes at 555 nm (ex) and 590 nm (em) using a fluorescence microplate reader (Molecular Devices). The initial turnover rates ($v0$) were calculated by fitting a linear regression line to the data for the first 0–60 seconds and then converted the resulting slopes expressed as RFU/second into $v0$ (nM/second) by using a conversion factor, 6.15 (RFU/nM), determined by experiments shown in Supplementary Fig. S1 (Supplementary Data are available online at www.liebertpub.com/nat).

TABLE 1. OLIGONUCLEOTIDES USED IN THIS STUDY

No.	*Sequence ID*	*Sequence*	T_m (°C)
1	**ApoB-20a**	5′-TTCAGcattggtattCAGTG-3′	76±0.4
2	**ApoB-20b**	5′-T°T°C°A°Gcattggtatt C°A°G°T°G-3′	79±0.6
3	**ApoB-20c**	5′-t°t°c°a°g°c°a°t°t°g°g°t°a°t°t°c°a°g°t°g-3′	59±0.6
4	**ApoB-16a**	5′-CAGcattggtatTCAG-3′	66±0.5
5	**ApoB-14a**	5′-AGCattggtatTCA-3′	62±0.6
6	**ApoB-14b**	5′-AgCattggtatTcA-3′	58±0.4
7	**ApoB-13a**	5′-GCattggtatTCA-3′	59±0.5
8	**ApoB-13b**	5′-G°CattggtatT°C°A-3′	62±0.1
9	**ApoB-13c**	5′-gCattGgtatTCA-3′	63±0.5
10	**ApoB-13d**	5′-GcattggtaTTCA-3′	58±0.8
11	**ApoB-13e**	5′-GCattggtattCA-3′	55±0.5
12	**ApoB-13f**	5′-G°CattggtattC°A-3′	57±0.1
13	**ApoB-13g**	5′-GCattggtatTcA-3′	58±0.6
14	**ApoB-13h**	5′-gcattggtatTCA-3′	48±0.7
15	**ApoB-13i**	5′-GCAttggtattca-3′	50±0.5
16	**ApoB-12a**	5′-GCattggtatTC-3′	52±0.6
17	**ApoB-12b**	5′-GCattggtaTtC-3′	53±0.5
18	**ApoB-12c**	5′-G°CattggtatT°C-3′	54±0.5
19	**ApoB-11a**	5′-CAttggtatTC-3′	39±0.5
20	**ApoB-11b**	5′-C°AttggtatT°C-3′	41±0.4
21	**ApoB-10a**	5′-CattggtatT-3′	28±0.4
22	**ApoB-10b**	5′-CAttggtaTT-3′	33±0.6
23	**ApoB-10c**	5′-C°AttggtaT°T-3′	36±0.5
24	**ApoB-10d**	5′-cattggtATT-3′	29±0.5
25	**DL-MRNA**	5′-R-*cacugaauaccaaugcugaa*-Q-3′	
26	**NL-MRNA**	5′-*cacugaauaccaaugcugaa*-3′	
27	**MRNA-1**	5′-*cacugaauac*-3′	
28	**MRNA-2**	5′-*caaugcugaa*-3′	

Upper case, *lower case*, *lower italic*, and *superscript circle* indicate locked nucleic acid (LNA), DNA, RNA, and phosphodiester linkage, respectively. All internucleotide linkages are phosphorothioated unless otherwise noted. All RNAs numbered 25, 26, 27, and 28 have phosphodiester internucleotide linkages. Melting temperatures (T_m) are shown as mean±SD.

apoB, apolipoprotein B-100; dl-mrna, dual-labeled complementary RNA probe; nl-mrna, non-labeled complementary 20-mer RNA.

In vivo *pharmacological experiments*

All animal procedures were performed in accordance with the guidelines of the Animal Care Ethics Committee of the National Cerebral and Cardiovascular Center Research Institute. All animal studies were approved by an institutional review board. All C57BL/6J mice (CLEA Japan) were male, and studies were initiated when animals were 8 weeks of age. Mice were maintained on a 12-hour light/12-hour dark cycle and fed *ad libitum*. Mice received a single treatment of AONs administered subcutaneously at a dose of 0.75 mg/kg. At the time of sacrifice, mice were anesthetized and livers were harvested and snap frozen until subsequent analysis. Whole blood was collected and subjected to serum separation for subsequent analysis.

mRNA quantification

Total RNA was isolated from mouse liver tissues using TRIzol Reagent (Life Technologies Japan) in accordance with the manufacturer's instructions. Gene expression was evaluated using a two-step quantitative reverse transcription-polymerase chain reaction (RT-PCR) method. Reverse transcription of RNA samples was performed using a High-Capacity cDNA Reverse-Transcription Kit (Life Technologies), and quantitative PCR was performed using TaqMan Gene Expression Assays (Life Technologies Japan). Messenger RNA levels of apoB were normalized against GAPDH mRNA levels. For murine apoB and GAPDH, TaqMan gene expression assays were used (assay IDs: Mm01545156_m1 and Mm99999915_g1, respectively).

AON quantification in liver

Assay was performed as described previously (Yamamoto et al., 2012a). Template DNA: 5′-gaatagcgatgaataccaatgc-3′ with biotin at the 3′ end; ligation probe DNA: 5′-tcgctattc-3′ with phosphate at the 5′ end and digoxigenin at the 3′ end.

Serum chemistry

Assay kits (#439-17501; WAKO) were used to measure serum levels of total cholesterol.

Statistics

Pharmacological studies were performed with more than three mice per treatment group. All data are expressed as means±standard deviation (SD). $P<0.05$ was considered to be statistically significant in all cases. Statistical comparisons were performed by Dunnett's or Bonferroni's multiple comparison tests.

Results and Discussion

Our first goal was to prepare bioactive AONs with a variety of binding affinities for the target RNA. We designed and

synthesized 24 AONs, as shown in Table 1. Most of the AONs were 10- to 20-mer LNA/DNA chimeras with full or partial PS backbones. DNA stretches on these AONs were kept in the 6- to 10-nt range, which is expected to be sufficient for eliciting RNase H of both *E. coli* and mammalian origins (Monia et al., 1993; Kurreck et al., 2002). ApoB-13c containing LNA in the center of the gap was prepared as a non-cleavable negative control. We next determined *T*m values of all AONs with the NL-MRNA (Table 1). As expected, *T*m values of these AONs were uniformly and broadly distributed from approximately 30° to 80°C under the indicated buffer conditions.

In order to investigate turnover activities of AONs, we developed a cell-free fluorescent turn-on system. DL-MRNA labeled with reporter dye (TAMRA) and quencher (BHQ2) on the 5′ and 3′ termini, respectively, was designed and prepared to detect RNA scission. Using this probe, we first evaluated the turnover activity of previously validated ApoB-13a. In the presence of an 80- to 240-fold molar excess of complementary RNA, 10 nM ApoB-13a was pre-incubated at 37°C in a 96-well microplate before addition of RNase H. It should be noted that the target complementary RNA used here consists of one-quarter dual-labeled DL-MRNA and three-quarters non-labeled NL-MRNA to avoid undesirable quenching or other interactions that may affect fluorescence (Supplementary Table S1). After addition of 60 units per well RNase H to the reactions, fluorescence intensities of TAMRA were measured (excitation = 555 nm and emission = 590 nm) every 15 seconds for 15 minutes (Supplementary Fig. S1A). Fluorescence of the reporter dye increased over time. The initial reaction rates also increased as a function of RNA concentration, where the initial reaction rates were determined from the slope of the initial linear portions (0–60 seconds) of the plots of fluorescence intensity versus time. In contrast, time-dependent fluorescence changes in TAMRA were not seen in an ApoB-13a-lacking control. We also observed very low background fluorescence levels in the control group, which indicates efficient quenching of TAMRA fluorescence by BHQ2, despite these dyes being 20 nt distant from one another. The fluorescence increases reached a plateau at 5 minutes. We confirmed that this indicates the completion of degradation of all target RNAs and then attempted to estimate the conversion coefficient between fluorescence intensity and concentration of RNA (Supplementary Figs. S1B, S2). By plotting fluorescence intensities at 15 minutes as a function of RNA concentration, we found high linear correlations between fluorescence intensity and concentration and determined 6.15 (RFU/nM) as a conversion factor. To determine the required amount of RNase H in this system, we performed further tests with various amounts of RNase H (2–180 units/well). A near maximum reaction rate could be obtained when at least 60 units/well of RNase H were added to the reaction, and confirmed that the rate-determining step of this reaction was not the scission step, but was the recycling step under these conditions (Supplementary Fig. S3). Taken together, these results are consistent with the recycling of ApoB-13a during this cell-free antisense reaction (see also Supplementary Fig. S4; Supplementary Table S2), and this system is useful for rapid screening of multiple-turnover activities of a series AONs.

We next aimed to measure a set of initial rates of AONs (Table 1). The initial velocities were determined as described above. At a concentration of 10 nM, each AON was incubated in the presence of 800 nM complementary RNA (DL-MRNA:NL-MRNA = 1:3) and 60 units/well RNase H. Time-dependent fluorescence changes were measured and initial rates were subsequently determined. The observed initial rates were rearranged in ascending order of *T*m values of corresponding AONs and are shown in Fig. 2A. As expected, we found an inverted U-shaped relationship between initial rate and *T*m values on the whole: AONs with high (> 60°C) and low (< 30°C) *T*m values have relatively small initial rates, while AONs having *T*m of 40°C–60°C showed efficient turnover in this system. This implies that AONs having higher multiple-turnover activities are more potent than conventional long LNA gapmers with extraordinarily high affinity. On the other hand, ApoB-12a showed the highest turnover ability among AONs tested, but ApoB-12a was shown to be less potent than ApoB-13a *in vivo* (Straarup et al., 2010). Thus, interpreting these data, we must take into account the differences between experimental buffer conditions used here and physiological conditions. For instance, it is known that longer PS-DNAs are more likely to form stronger undesirable complexes with proteins and inactivate RNase H to reduce their efficacy (Gao et al., 1992; Watanabe et al., 2006). As in this system, there are limited accompanying components such as inorganics, proteins, and lipids, and effects including such length-dependent factors may not have been considered. Among the four 10-mer LNAs, ApoB-10a and ApoB-10d showed marked inefficient turnover activity when compared with ApoB-10b and ApoB-10c, indicating a lack of binding affinity. In contrast, the two 20-mer AONs showed inefficient turnover activities when compared with ApoB-20c, probably due to slow product release.

Surprisingly, turnover activities of ApoB-13d and ApoB-13h were exceptionally low, although their *T*m values were in an active range (Fig. 2A). To better understand this observation, we further measured *T*m values of AONs with two additional 10-mer RNAs (MRNA-1, MRNA-2) (Fig. 2B). MRNA-1 and MRNA-2 were prepared as models for the cleaved products of RNase H and correspond to the 5′ and 3′ halves of NL-MRNA, respectively. The results showed that melting temperatures for MRNA-1 were lower than those for MRNA-2, but this trend was reversed in ApoB-13d and ApoB-13h. This potential affinity bias may explain the difference in efficiency of turnover activity. The consensus sequence for the preferred RNase H cleavage sites is unknown; instead, a strong positional preference for cleavage has been observed in a family of enzymes. For example, human RNase H1 has been shown to preferentially cleave the RNA part of RNA/DNA hybrid several nucleotides away from the 5′-RNA/3′-DNA terminus, probably due to the binding directionality of the enzyme (Lima et al., 2007a; Lima et al., 2007b). It has been predicted that the hybrid binding domain of RNase H binds the 5′-RNA/3′-DNA flank of the hybrid relative to the catalytic domain, which is strongly supported by the crystal structure of human RNase H with RNA/DNA hybrids (Nowotny et al., 2007). Despite some reported differences between *E. coli* and human RNase H such as a minimal gap size required for activation of RNase H (Monia et al., 1993; Crooke et al., 1995), the high similarity of the structures of human RNase H1 and *E. coli* RNase H1 suggests that this positional directionality for cleavage encourages ApoB-13d to produce longer RNA segments than fragments

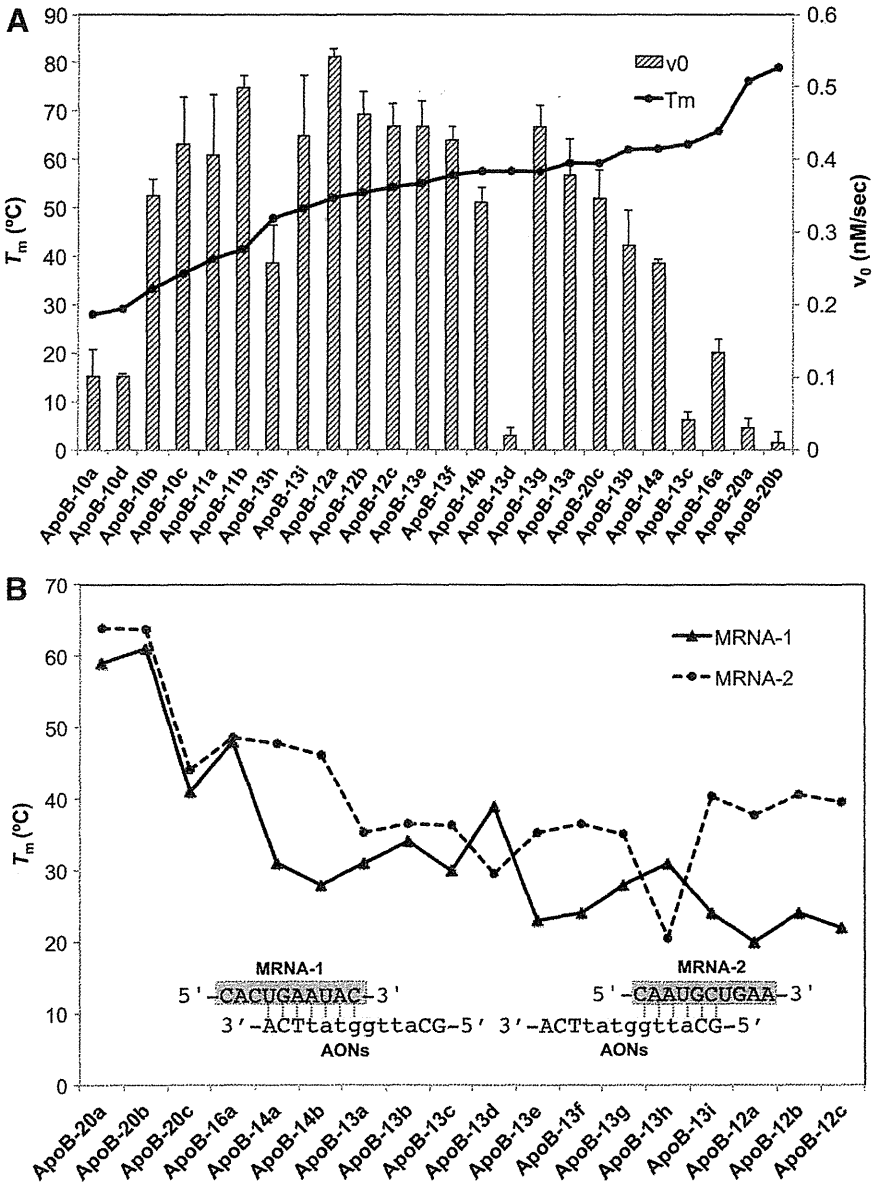

FIG. 2. **(A)** Relationship between turnover rate and gross or local affinity. Initial rates (v_0, bar graph) of turnover reaction rearranged in ascending order of melting temperature (T_m) values (*black line*) of corresponding antisense oligonucleotides (AONs). Data are means ± standard deviation (SD). **(B)** Melting temperatures with MRNA-1 (*solid*) and MRNA-2 (*dotted*). All experiments here were repeated at least three times. Color images available online at www.liebertpub.com/nat

produced by other AONs, thereby forming very stable duplexes with the 3′ half of ApoB-13d and eventually decelerating product release, as well as turnover. Collectively, the requirements for high turnover rates would be adequate binding affinity of the duplex formed by using several bases of AON (for the rapid release of cleaved mRNA), as well as moderate binding affinity of full-length AON/mRNA duplex (for efficient target capture). In contrast, the affinity of the 5′ half of ApoB-13h is thought to be too low to form stable duplexes for cleavage.

In order to explore the capacity of turnover under biological conditions, we attempted to evaluate the *in vivo* efficacy of AONs with identical length (ApoB-13a, -13d, -13e, -13g, and -13h), and to compare the *T*m data relevant to turnover activity. We here adopted a low dosage of 0.75 mg kg^{-1}, which had been confirmed as being sufficient to achieve knockdown of the target apoB mRNA for ApoB-13a, a positive control for *in vivo* screening, because even a single administration of a relatively low dose of 5 mg/kg ApoB-13a had been shown to reduce apoB mRNA by 97%, which made it difficult to discriminate differences in efficacy when AONs screened have similar high efficacy (Straarup et al., 2010). Mice ($n = 3$/group) were dosed subcutaneously with 0.75 mg kg^{-1} ApoB-13a, -13d, -13e, -13g and -13h. After 48 hours post-injection, expression levels of apoB mRNA in the liver were analyzed. The apoB mRNA reduction is associated with the clinically relevant therapeutic phenotype characterized by reduced blood cholesterol concentration for the treatment of hypercholesterolemia. Expression levels were rearranged in ascending order of *T*m values of corresponding AONs vs full-length NL-MRNA and are described in Fig. 3. The highest level of reduction in hepatic apoB mRNA was observed in ApoB-13a, while the lowest level of reduction was observed in ApoB-13d and -13h (Fig. 3A; Supplementary Table S3). Statistical significance was seen for ApoB-13a, -13e and -13g, but not for ApoB-13d and -13h. A similar-sized LNA phosphorothioate oligonulecotide without target sites on apoB mRNA was used as a control, showing no decrease in

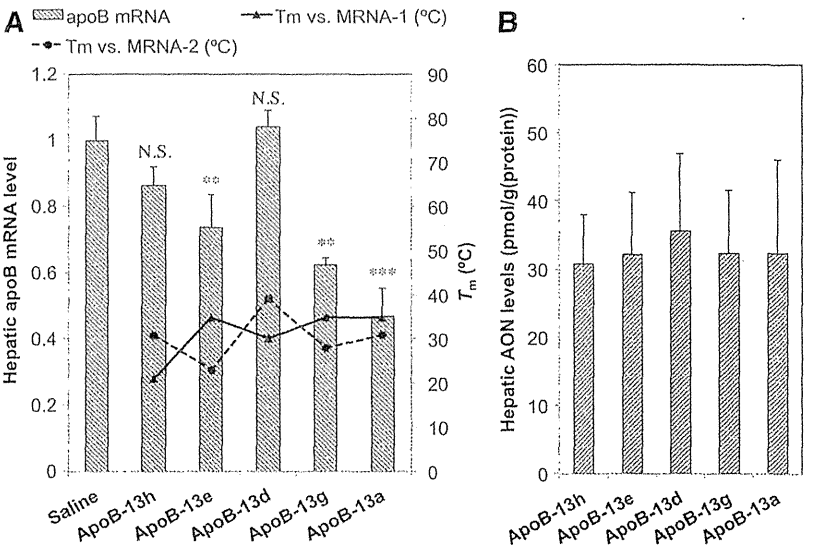

FIG. 3. Reduction of apoB mRNA in the livers (bar graph) of mice ($n=3$/group) receiving a single subcutaneous dose of 0.75 mg kg^{-1} of a series of 13-mer AONs **(A)** rearranged in ascending order of T_m values along with melting temperatures versus MRNA-1 (*solid*) and MRNA-2 (*dashed*). Dunnett's multiple comparison test, $***p<0.001$; $**p<0.01$; N.S., not significant. **(B)** The mouse liver content of a series of 13-mer AONs. Bonferroni multiple comparison tests did not reveal any of arms to be significantly different across groups, $p<0.05$. Error bars represent group means + SD $n=3$.

hepatic apoB mRNA and no potential toxicity (Supplementary Tables S3, S4).

The efficacy order of ApoB-13a > -13g > -13e > -13h > -13d appears to be unrelated to binding affinity to full-length NL-MRNA, but inefficiency of ApoB-13d and ApoB-13h *in vivo* were consistent with their slow turnover rates in the cell-free system, while other AONs are potent *in vivo* and show fast turnover rates in the cell-free system. Serum reduction levels in total cholesterol denoted the same tendency as mRNA reduction levels (Supplementary Fig. S5). As we selected AONs with an identical length of 13 nt, identical sequences and similar compositions for *in vivo* examination, the mouse liver content of these 13-mer AONs was measured and found to be almost identical (Fig. 3B). In addition to this, we speculate that AONs are not necessarily in vast excess of mRNA even *in vivo*. Sohlenius-Sternbeck has estimated a hepatocellularity number for humans, mice and other animal livers (Sohlenius-Sternbeck, 2006). The value for mice was estimated to be 135×10^6 cells per gram of liver, where livers of 8-week-old mice are 1.0 gram on average. On the other hand, we and others have calculated that approximately <10% of dosed oligonucleotides (<400 pmol for 0.75 mg/kg) reside in liver, even at 48–72 h post-dosing (Straarup et al., 2010; Yamamoto et al., 2012a).

Considering these conditions, each parenchymal cell may be exposed to AONs to a lesser extent than it is in a conventional *in vitro* transfection experiment. Furthermore, nonparenchymal cells such as Kupffer cells are thought to be more likely to ingest AONs than apoB-expressing parenchymal cells do and intracellular distribution of AONs *via* non-productive uptake further reduces the active form of AONs (Koller et al., 2011). In the light of this context, our *in vivo* multiple-turnover hypothesis is a compelling explanation for the *in vivo* activity of AONs. Of course, as there may exist differences such as intracellular distribution of AONs into productive versus less productive compartments, which can be influenced by small changes in chemistry and protein binding ability, it is necessary to continue gathering evidence. This hypothesis may also offer a new direction with regard to the remaining issues in antisense drug development; for example, inconsistency between *in vitro* gene silencing activity of AONs delivered in complex with transfection vehicles and *in vivo* activity of naked AONs (Stein et al., 2010; Zhang et al., 2011).

In the presence of transfection reagents, AONs are delivered quite efficiently to reaction sites, and consequently, might be placed under single-turnover conditions, while inefficient naked conditions may encourage multiple-turnover conditions. However, it should again be noted that it is difficult to monitor the intracellular turnover reaction in living cells and tissues due to their dynamic nature; thus, further experimental support is necessary to determine whether AONs are actually placed under multiple-turnover conditions at the intracellular antisense reaction site. Nevertheless, our study provides an important opportunity to shed light on the uncertain antisense mechanisms, and may lead to further improvement of the activity and safety profiles of AONs.

Acknowledgments

This work was supported by JSPS KAKENHI grant number 24890102 and the Advanced Research for Medical Products Mining Programme of the National Institute of Biomedical Innovation (NIBIO).

Author Disclosure Statement

No competing financial interests exist.

References

CROOKE, S.T., LEMONIDIS, K.M., NEILSON, L., GRIFFEY, R., LESNIK, E.A., and MONIA, B.P. (1995). Kinetic characteristics of Escherichia coli RNase H1: cleavage of various antisense oligonucleotide-RNA duplexes. Biochem. J. **312,** 599–608.

CROOKE, T.S. (2007). Antisense Drug Technologies: Principles, Strategies, and Applications. 2nd ed. (CRC Press Taylor & Francis Group, Boca Raton, FL).

GAO, W.Y., HAN, F.S., STORM, C., EGAN, W., and CHENG, Y.C. (1992). Phosphorothioate oligonucleotides are inhibitors of human DNA polymerases and RNase H: implications for antisense technology. Mol. Pharmacol. **41,** 223–229.

HARI, Y., OBIKA, S., OHNISHI, R., EGUCHI, K., OSAKI, T., OHISHI, H., and IMANISHI, T. (2006). Synthesis and properties of 2′-O,4-C-methyleneoxymethylene bridged nucleic acid. Bioorgan. Med. Chem. **14,** 1029–1038.

HUTVAGNER, G., and ZAMORE, P.D. (2002). A microRNA in a multiple-turnover RNAi enzyme complex. Science **297,** 2056–2060.

KOLLER, E., VINCENT, T. M., CHAPPELL, A., DE, S., MANOHARAN, M., and BENNETT, C. F. (2011). Mechanisms of single-stranded phosphorothioate modified antisense oligonucleotide accumulation in hepatocytes. Nucleic Acids Res. **39,** 4795–4807.

KURRECK, J., WYSZKO, E., GILLEN, C., and ERDMANN, V.A. (2002). Design of antisense oligonucleotides stabilized by locked nucleic acids. Nucleic Acids Res. **30,** 1911–1918.

LIMA, W.F., and CROOKE, S.T. (1997). Binding affinity and specificity of Escherichia coli RNase H1: impact on the kinetics of catalysis of antisense oligonucleotide-RNA hybrids. Biochemistry **36,** 390–398.

LIMA, W.F., ROSE, J.B., NICHOLS, J.G., WU, H.J., MIGAWA, M.T., WYRZYKIEWICZ, T.K., SIWKOWSKI, A.M., and CROOKE, S.T. (2007a). Human RNase H1 discriminates between subtle variations in the structure of the heteroduplex substrate. Mol. Pharmacol. **71,** 83–91.

LIMA, W.F., ROSE, J.B., NICHOLS, J.G., WU, H.J., MIGAWA, M.T., WYRZYKIEWICZ, T.K., VASQUEZ, G., SWAYZE, E.E., and CROOKE, S.T. (2007b). The positional influence of the helical geometry of the heteroduplex substrate on human RNase H1 catalysis. Mol. Pharmacol. **71,** 73–82.

MIYASHITA, K., RAHMAN, S.M.A., SEKI, S., OBIKA, S., and IMANISHI, T. (2007). *N*-Methyl substituted 2′,4′-BNA^{NC}: a highly nuclease-resistant nucleic acid analogue with high-affinity RNA selective hybridization. Chem. Commun. **2007,** 3765–3767.

MONIA, B.P., LESNIK, E.A., GONZALEZ, C., LIMA, W.F., MCGEE, D., GUINOSSO, C.J., KAWASAKI, A.M., COOK, P.D., and FREIER, S.M. (1993). Evaluation of 2′-modified oligonucleotides containing 2′-deoxy gaps as antisense inhibitors of gene expression. J. Biol. Chem. **268,** 14514–14522.

NOWOTNY, M., GAIDAMAKOV, S.A., GHIRLANDO, R., CERRITELLI, S.M., CROUCH, R.J., and YANG, W. (2007). Structure of human RNase h1 complexed with an RNA/DNA hybrid: insight into HIV reverse transcription. Mol. Cell **28,** 264–276.

OBIKA, S., NANBU, D., HARI, Y., ANDOH, J., MORIO, K., DOI, T., and IMANISHI, T. (1998). Stability and structural features of the duplexes containing nucleoside analogues with a fixed N-type conformation, 2′-*O*,4′-*C*-methyleneribonucleosides. Tetrahedron Lett. **39,** 5401–5404.

OBIKA, S., NANBU, D., HARI, Y., MORIO, K., IN, Y., ISHIDA, T., and IMANISHI, T. (1997). Synthesis of 2′-O,4′-C-methyleneuridine and -cytidine. Novel bicyclic nucleosides having a fixed C-3,-endo sugar puckering. Tetrahedron Lett. **38,** 8735–8738.

PRAKASH, T.P., SIWKOWSKI, A., ALLERSON, C.R., MIGAWA, M.T., LEE, S., GAUS, H.J., BLACK, C., SETH, P.P., SWAYZE, E.E., and BHAT, B. (2010). Antisense oligonucleotides containing conformationally constrained 2′,4′-(N-methoxy)aminomethylene and 2′,4′-aminooxymethylene and 2′-O,4′-C-aminomethylene bridged nucleoside analogues show improved potency in animal models. J. Med. Chem. **53,** 1636–1650.

SETH, P.P., SIWKOWSKI, A., ALLERSON, C.R., VASQUEZ, G., LEE, S., PRAKASH, T.P., WANCEWICZ, E.V., WITCHELL, D., and SWAYZE, E.E. (2009). Short antisense oligonucleotides with novel 2′-4′ conformationaly restricted nucleoside analogues show improved potency without increased toxicity in animals. J. Med. Chem. **52,** 10–13.

SINGH, S.K., NIELSEN, P., KOSHKIN, A.A., and WENGEL, J. (1998). LNA (locked nucleic acids): synthesis and high-affinity nucleic acid recognition. Chem. Commun. **1998,** 455–456.

SOHLENIUS-STERNBECK, A.K. (2006) Determination of the hepatocellularity number for human, dog, rabbit, rat and mouse livers from protein concentration measurements. Toxicol. In Vitro **20,** 1582–1586.

STANTON, R., SCIABOLA, S., SALATTO, C., WENG, Y., MOSHINSKY, D., LITTLE, J., WALTERS, E., KREEGER, J., et al. (2012). Chemical modification study of antisense gapmers. Nucleic Acid Ther. **22,** 344–359.

STEIN, C.A., HANSEN, J.B., LAI, J., WU, S., VOSKRESENSKIY, A., HOG, A., WORM, J., HEDTJARN, M., SOULEIMANIAN, N., MILLER, P., et al. (2010). Efficient gene silencing by delivery of locked nucleic acid antisense oligonucleotides, unassisted by transfection reagents. Nucleic Acids Res. **38,** e3.

STRAARUP, E.M., FISKER, N., HEDTJARN, M., LINDHOLM, M.W., ROSENBOHM, C., AARUP, V., HANSEN, H.F., ORUM, H., HANSEN, J.B., and KOCH, T. (2010). Short locked nucleic acid antisense oligonucleotides potently reduce apolipoprotein B mRNA and serum cholesterol in mice and non-human primates. Nucleic Acids Res. **38,** 7100–7111.

VESTER, B., BOEL, A.M., LOBEDANZ, S., BABU, B.R., RAUNKJAER, M., LINDEGAARD, D., RAUNAK, HRDLICKA, P.J., HOJLAND, T., et al. (2008). Chemically modified oligonucleotides with efficient RNase H response. Bioorg. Med. Chem. Lett. **18,** 2296–2300.

WATANABE, T.A., GEARY, R.S., and LEVIN, A.A. (2006). Plasma protein binding of an antisense oligonucleotide targeting human ICAM-1 (ISIS 2302). Oligonucleotides **16,** 169–180.

YAHARA, A., SHRESTHA, A.R., YAMAMOTO, T., HARI, Y., OSAWA, T., YAMAGUCHI, M., NISHIDA, M., KODAMA, T., and OBIKA, S. (2012). Amido-bridged nucleic acids (AmNAs): synthesis, duplex stability, nuclease resistance, and in vitro antisense potency. Chembiochem **13,** 2513–2516.

YAMAMOTO, T., HARADA-SHIBA, M., NAKATANI, M., WADA, S., YASUHARA, H., NARUKAWA, K., SASAKI, K., SHIBATA, M.A., TORIGOE, H., et al. (2012a). Cholesterol-lowering action of BNA-based antisense oligonucleotides targeting PCSK9 in atherogenic diet-induced hypercholesterolemic mice. Mol. Ther. Nucleic Acids **1,** e22.

YAMAMOTO, T., NAKATANI, M., NARUKAWA, K., and OBIKA, S. (2011). Antisense drug discovery and development. Future Med. Chem. **3,** 339–365.

YAMAMOTO, T., YASUHARA, H., WADA, F., HARADA-SHIBA, M., IMANISHI, T., and OBIKA, S. (2012b). Superior silencing by 22,42-BNA^{NC}-Based short antisense oligonucleotides compared to 22,42-BNA/LNA-based apolipoprotein B antisense inhibitors. J. Nucleic Acids, Article ID 707323.

ZHANG, Y., QU, Z., KIM, S., SHI, V., LIAO, B., KRAFT, P., BANDARU, R., WU, Y., GREENBERGER, L.M., and HORAK, I.D. (2011). Down-modulation of cancer targets using locked nucleic acid (LNA)-based antisense oligonucleotides without transfection. Gene Ther, **18,** 326–333.

Address correspondence to:
Satoshi Obika, PhD
Graduate School of Pharmaceutical Sciences
Osaka University
1-6 Yamadaoka
Suita, Osaka 565-0871
Japan

E-mail: obika@phs.osaka-u.ac.jp

Received for publication October 23, 2013; accepted after revision March 13, 2014.

Volume 723 15 January 2014 ISSN 0014-2999

european journal of pharmacology

Drugs in Action

ELSEVIER

European Journal of Pharmacology 723 (2014) 353–359

Contents lists available at ScienceDirect

European Journal of Pharmacology

journal homepage: www.elsevier.com/locate/ejphar

Cardiovascular Pharmacology

Locked nucleic acid antisense inhibitor targeting apolipoprotein C-III efficiently and preferentially removes triglyceride from large very low-density lipoprotein particles in murine plasma

Tsuyoshi Yamamoto [a,b], Satoshi Obika [a,**], Moeka Nakatani [a,b], Hidenori Yasuhara [a,b], Fumito Wada [a,b], Eiko Shibata [a,b,c], Masa-Aki Shibata [c], Mariko Harada-Shiba [b,*]

[a] Graduate School of Pharmaceutical Sciences, Osaka University, 1-6 Yamadaoka, Suita, Osaka 565-0871, Japan
[b] Department of Molecular Innovation in Lipidology, National Cerebral and Cardiovascular Center Research Institute, 5-7-1 Fujishirodai, Suita, Osaka 565-8565, Japan
[c] Graduate School of Health Sciences, Osaka Health Science University, Osaka, Japan

ARTICLE INFO

Article history:
Received 23 May 2013
Received in revised form
25 October 2013
Accepted 2 November 2013
Available online 20 November 2013

Keywords:
Hyperlipidemia
Antisense oligonucleotide
Synthetic nucleic acid
Bridged nucleic acids
Locked nucleic acids
Apolipoprotein C-III

ABSTRACT

A 20-mer phosphorothioate antisense oligodeoxyribonucleotide having locked nucleic acids (LNA–AON) was used to reduce elevated serum triglyceride levels in mice. We repeatedly administered LNA–AON, which targets murine apolipoprotein C-III mRNA, to high-fat-fed C57Bl/6J male mice for 2 weeks. The LNA–AON showed efficient dose-dependent reductions in hepatic apolipoprotein C-III mRNA and decreased serum apolipoprotein C-III protein concentrations, along with efficient dose-dependent reductions in serum triglyceride concentrations and attenuation of fat accumulation in the liver. Through precise lipoprotein profiling analysis of sera, we found that serum reductions in triglyceride and cholesterol levels were largely a result of decreased serum very low-density lipoprotein (VLDL)-triglycerides and -cholesterol. It is noteworthy that larger VLDL particles were more susceptible to removal from blood than smaller particles, resulting in a shift in particle size distribution to smaller diameters. Histopathologically, fatty changes were markedly reduced in antisense-treated mice, while moderate granular degeneration was frequently seen the highest dose of LNA–AON. The observed granular degeneration of hepatocytes may be associated with moderate elevation in the levels of serum transaminases. In conclusion, we developed an LNA-based selective inhibitor of apolipoprotein C-III. Although it remains necessary to eliminate its potential hepatotoxicity, the present LNA–AON will be helpful for further elucidating the molecular biology of apolipoprotein C-III.

1. Introduction

Apolipoprotein C-III (apoC-III) is synthesized mainly in the liver and circulates in plasma (Bruns et al., 1984). The mechanism of apoC-III action is primarily thought to be the attenuation of hydrolysis of triglycerides in lipoproteins, principally by inhibiting capillary endothelial lipoprotein lipase activity. Thus, serum accumulation of apoC-III would cause reduced clearance of triglyceride-rich lipoprotein particles from blood, resulting in the blood accumulation of triglyceride-rich lipoproteins (Havel et al., 1973; Wang et al., 1985). ApoC-III is also known to reduce the clearance of triglyceride-rich lipoproteins and their remnants by blocking apolipoprotein B- or apolipoprotein E-mediated uptake of these lipoproteins to low-density lipoprotein (LDL) receptor (Clavey et al., 1995; Sehayek and Eisenberg, 1991). As growing evidence has shown that elevated plasma triglyceride levels are major risk factors for metabolic syndrome, type 2 diabetes and cardiovascular diseases, apoC-III is a potential therapeutic target for these diseases (Goldberg, 2001; Grundy et al., 2004; Hokanson and Austin, 1996; Sarwar et al., 2007). This notion is also supported by the observation that humans with a null mutation in *APOC3* gene show lower fasting and postprandial serum triglycerides and LDL cholesterol and higher high-density lipoprotein (HDL) cholesterol levels, as well as reduced coronary artery calcification, as compared to humans with normal apoC-III activity (Pollin et al., 2008), while some specific single-nucleotide polymorphism carriers in *APOC3* show increased plasma triglyceride levels and evidence of non-alcoholic fatty liver, in addition to

* Corresponding author. Tel.: +81 6 6833 5012x8209; fax: +81 6 6872 7485.
** Corresponding author. Tel.: +81 6 6879 8200; fax: +81 6 6879 8204.
E-mail addresses: t-yam@phs.osaka-u.ac.jp (T. Yamamoto), obika@phs.osaka-u.ac.jp (S. Obika), moeka6287@gmail.com (M. Nakatani), yasuhara-h@phs.osaka-u.ac.jp (H. Yasuhara), wada.fumito.ri@ncvc.go.jp (F. Wada), belleiko@ncvc.go.jp (E. Shibata), masaaki.shibata@ohsu.ac.jp (M.-A. Shibata), mshiba@ncvc.go.jp (M. Harada-Shiba).

0014-2999/$ - see front matter © 2013 Elsevier B.V. All rights reserved.
http://dx.doi.org/10.1016/j.ejphar.2013.11.004

European Journal of Pharmacology 723 (2014) 353–359

Contents lists available at ScienceDirect

European Journal of Pharmacology

journal homepage: www.elsevier.com/locate/ejphar

Cardiovascular Pharmacology

Locked nucleic acid antisense inhibitor targeting apolipoprotein C-III efficiently and preferentially removes triglyceride from large very low-density lipoprotein particles in murine plasma

Tsuyoshi Yamamoto [a,b], Satoshi Obika [a,**], Moeka Nakatani [a,b], Hidenori Yasuhara [a,b], Fumito Wada [a,b], Eiko Shibata [a,b,c], Masa-Aki Shibata [c], Mariko Harada-Shiba [b,*]

[a] Graduate School of Pharmaceutical Sciences, Osaka University, 1-6 Yamadaoka, Suita, Osaka 565-0871, Japan
[b] Department of Molecular Innovation in Lipidology, National Cerebral and Cardiovascular Center Research Institute, 5-7-1 Fujishirodai, Suita, Osaka 565-8565, Japan
[c] Graduate School of Health Sciences, Osaka Health Science University, Osaka, Japan

ARTICLE INFO

Article history:
Received 23 May 2013
Received in revised form
25 October 2013
Accepted 2 November 2013
Available online 20 November 2013

Keywords:
Hyperlipidemia
Antisense oligonucleotide
Synthetic nucleic acid
Bridged nucleic acids
Locked nucleic acids
Apolipoprotein C-III

ABSTRACT

A 20-mer phosphorothioate antisense oligodeoxyribonucleotide having locked nucleic acids (LNA–AON) was used to reduce elevated serum triglyceride levels in mice. We repeatedly administered LNA–AON, which targets murine apolipoprotein C-III mRNA, to high-fat-fed C57Bl/6J male mice for 2 weeks. The LNA–AON showed efficient dose-dependent reductions in hepatic apolipoprotein C-III mRNA and decreased serum apolipoprotein C-III protein concentrations, along with efficient dose-dependent reductions in serum triglyceride concentrations and attenuation of fat accumulation in the liver. Through precise lipoprotein profiling analysis of sera, we found that serum reductions in triglyceride and cholesterol levels were largely a result of decreased serum very low-density lipoprotein (VLDL)-triglycerides and -cholesterol. It is noteworthy that larger VLDL particles were more susceptible to removal from blood than smaller particles, resulting in a shift in particle size distribution to smaller diameters. Histopathologically, fatty changes were markedly reduced in antisense-treated mice, while moderate granular degeneration was frequently seen the highest dose of LNA–AON. The observed granular degeneration of hepatocytes may be associated with moderate elevation in the levels of serum transaminases. In conclusion, we developed an LNA-based selective inhibitor of apolipoprotein C-III. Although it remains necessary to eliminate its potential hepatotoxicity, the present LNA–AON will be helpful for further elucidating the molecular biology of apolipoprotein C-III.

1. Introduction

Apolipoprotein C-III (apoC-III) is synthesized mainly in the liver and circulates in plasma (Bruns et al., 1984). The mechanism of apoC-III action is primarily thought to be the attenuation of hydrolysis of triglycerides in lipoproteins, principally by inhibiting capillary endothelial lipoprotein lipase activity. Thus, serum accumulation of apoC-III would cause reduced clearance of triglyceride-rich lipoprotein particles from blood, resulting in the blood accumulation of triglyceride-rich lipoproteins (Havel et al., 1973; Wang et al., 1985). ApoC-III is also known to reduce the clearance of triglyceride-rich lipoproteins and their remnants by blocking apolipoprotein B- or apolipoprotein E-mediated uptake of these lipoproteins to low-density lipoprotein (LDL) receptor (Clavey et al., 1995; Sehayek and Eisenberg, 1991). As growing evidence has shown that elevated plasma triglyceride levels are major risk factors for metabolic syndrome, type 2 diabetes and cardiovascular diseases, apoC-III is a potential therapeutic target for these diseases (Goldberg, 2001; Grundy et al., 2004; Hokanson and Austin, 1996; Sarwar et al., 2007). This notion is also supported by the observation that humans with a null mutation in *APOC3* gene show lower fasting and postprandial serum triglycerides and LDL cholesterol and higher high-density lipoprotein (HDL) cholesterol levels, as well as reduced coronary artery calcification, as compared to humans with normal apoC-III activity (Pollin et al., 2008), while some specific single-nucleotide polymorphism carriers in *APOC3* show increased plasma triglyceride levels and evidence of non-alcoholic fatty liver, in addition to

* Corresponding author. Tel.: +81 6 6833 5012x8209; fax: +81 6 6872 7485.
** Corresponding author. Tel.: +81 6 6879 8200; fax: +81 6 6879 8204.
E-mail addresses: t-yam@phs.osaka-u.ac.jp (T. Yamamoto), obika@phs.osaka-u.ac.jp (S. Obika), moeka6287@gmail.com (M. Nakatani), yasuhara-h@phs.osaka-u.ac.jp (H. Yasuhara), wada.fumito.ri@ncvc.go.jp (F. Wada), belleiko@ncvc.go.jp (E. Shibata), masaaki.shibata@ohsu.ac.jp (M.-A. Shibata), mshiba@ncvc.go.jp (M. Harada-Shiba).

0014-2999/$ - see front matter © 2013 Elsevier B.V. All rights reserved.
http://dx.doi.org/10.1016/j.ejphar.2013.11.004

elevated cardiovascular disease risk (Petersen et al., 2010). A number of studies using genetically engineered mouse models have also revealed the dyslipidemic or atherogenic effects of apoC-III (Gerritsen et al., 2005; Ito et al., 1990; Jong et al., 2001; Takahashi et al., 2003). In addition, attenuation of apoC-III has been shown to be beneficial for type I diabetes (Holmberg et al., 2011; Juntti-Berggren et al., 1993, 2004). Thus, the privation of apoC-III would lead to significant benefits, both indirectly and directly, in the reduction of cardiovascular disease risk (Ooi et al., 2008; Pollin et al., 2008).

There are currently several state-of-the-art gene silencing approaches available for target-specific disruption, such as antisense oligonucleotides (AONs), monoclonal antibodies and small interfering RNAs (siRNAs), which are showing promising results, particularly in dyslipidemia therapy (Norata et al., 2013). Graham et al. (2013) recently reported successful attenuation of apoC-III mRNA and plasma triglyceride levels in preclinical models and humans by using antisense oligonucleotides chemically modified with 2′-*O*-methoxyethyl RNAs, which are known to preferentially distribute to the liver, where apoC-III is synthesized (Graham et al., 2013). Our group has developed a series of conformationally constrained nucleic acids including 2′,4′-bridged nucleic acids (2′,4′-BNAs), which are also known as locked nucleic acids (LNAs) (Mitsuoka et al., 2009; Miyashita et al., 2007; Obika et al., 1997; Yahara et al., 2012). This class of modified nucleotides has been found to have superior potential for antisense therapeutics on account of their extraordinarily high mRNA binding, as well as systemic effects over 2′-*O*-methoxyethyl RNAs (Gupta et al., 2010; Lanford et al., 2010; Lindholm et al., 2012; Prakash et al., 2010; Seth et al., 2009; Yamamoto et al., 2012). Specifically, the in vivo potencies of LNA-based AONs are generally 5 to 10-fold greater than their 2′-*O*-methoxyethyl RNA-containing counterparts (Prakash et al., 2010; Seth et al., 2009). Thus, LNA-based anti-apoC-III AONs are expected to be better alternatives to 2′-*O*-methoxyethyl RNA-containing congeners. We here demonstrated the effective reduction in elevated serum triglyceride levels in mice using LNA-based AONs targeting hepatic apoC-III mRNA.

2. Materials and methods

2.1. Antisense oligonucleotides

LNA was partially incorporated into a 20-mer phosphorothioated oligodeoxyribonucleotide. We prepared two potential AONs, **A301S** (5′-tcttatccagctttattagg-3′) and **A301SL** (5′-TCtTaTCcagcttTaTTaGg-3′), in which lowercase and uppercase letters represent DNA and LNA, respectively. These AONs have an identical sequence targeting murine apoC-III mRNA, a sequence patented by ISIS pharmaceuticals as being highly potent (Crooke et al., 2009). These modified AONs were synthesized and provided by Gene Design (Osaka, Japan). Syntheses were conducted using standard phosphoramidite procedures, and products were carefully processed under aseptic conditions and purified. All products were endotoxin-free and contained low levels of residual salts for in vivo usage.

2.2. In vivo pharmacological experiments

All animal procedures were performed in accordance with the guidelines of the Animal Care Ethics Committee of the National Cerebral and Cardiovascular Center Research Institute (Osaka, Japan). All animal studies were approved by the Institutional Review Board. C57BL/6J mice were obtained from CLEA Japan (Tokyo, Japan). All mice were male, and studies were initiated when animals were aged 6–8 weeks. Mice were maintained on a 12-h light/12-h dark cycle and fed ad libitum. Mice were fed normal chow (CE-2; CLEA Japan) or Western diet (F2WTD; Oriental Yeast, Tokyo, Japan) for 2 weeks before the first treatment and throughout the experimental period. Mice received multiple treatments with AONs administered intraperitoneally at doses of 10 and 20 mg/kg/injection. Peripheral blood was collected from the tail vein in BD Microtainers (BD, Franklin Lakes, NJ) for separation of serum. At the time of sacrifice, livers were harvested and snap frozen until subsequent analysis. Collected blood was subjected to serum separation for subsequent analysis.

2.3. High performance liquid chromatography analysis of serum

The cholesterol and triglyceride profiles of serum lipoproteins were analyzed using a dual detection high performance liquid chromatography (HPLC) system with two tandem connected TSKgel LipopropakXL columns (300 mm × 7.8 mm; Tosoh, Tokyo, Japan), in accordance with the methods provided by Skylight Biotech (Akita, Japan). Individual subfractions were quantified by best curve fitting analysis, assuming that the particle sizes of all subfractions followed a Gaussian distribution. Particle sizes for individual subfractions were previously determined as 44.5–64 nm (large VLDL), 36.8 nm (medium VLDL), 31.3 nm (small VLDL), 28.6 nm (large LDL), 25.5 nm (medium LDL), 23 nm (small LDL), 16.7–20.7 nm (very small LDL), 13.5–15 nm (very large HDL), 12.1 nm (large HDL), 10.9 nm (medium HDL), 9.8 nm (small HDL) and 7.6–8.8 nm (very small HDL) (Okazaki et al., 2005; Usui et al., 2002).

2.4. mRNA quantification

Total RNA was isolated from cultured cells or mouse liver tissues using TRIzol Reagent (Life Technologies Japan, Tokyo, Japan) according to the manufacturer's protocols. Gene expression was evaluated by 2-step quantitative reverse transcription PCR (RT-PCR). Reverse-transcription of RNA samples was performed using a High Capacity cDNA Reverse-Transcription Kit (Life Technologies Japan, Tokyo, Japan), and quantitative PCR was performed by TaqMan Gene Expression Assay (Life Technologies Japan, Tokyo, Japan). mRNA levels of target genes were normalized against glyceraldehyde-3-phosphate dehydrogenase (GAPDH) mRNA levels. The following primer sets were used for quantitative PCR: for assay ID, Mm00445670_m1 (apoc3) and Mm99999915_m1 (gapdh).

2.5. Western blotting analysis

Serum was diluted with buffer (150 mM NaCl, 1.0% IGEPAL® CA-630, 0.5% sodium deoxycholate, 0.1% SDS, 50 mM Tris, pH 8.0, 20 × Complete Mini protease inhibitor cocktail 1:20 (Roche, Indianapolis, IN)) and total protein concentrations were measured with a detergent compatible assay kit (Bio-Rad, Hercules, CA). Solutions were subjected to electrophoresis on 16% Tris-glycine gels (Life Technologies Japan, Tokyo, Japan) at 180 V for 30 min, and were transferred to a PVDF membrane (Bio-Rad). Apo-CIII Western blotting was performed at room temperature for 1 h with an anti-apo-CIII antibody (Santa Cruz Biotechnology, Santa Cruz, CA) at 200 mV for 120 min. Membranes were washed three times with PBS containing 0.3% Tween20. Blots were labeled with horseradish peroxidase-conjugated secondary goat anti-rabbit antibody (Santa Cruz Biotechnology, Santa Cruz, CA). Chemiluminescent detection was performed using an ECL prime Western blot detection kit (Amersham Biosciences, Buckinghamshire, UK), and bands were visualized using an LAS-4000 mini image analyzer (Fuji Film, Tokyo, Japan).

2.6. Serum chemistry and histopathology

Blood collected from the inferior vena cava upon sacrifice was subjected to serum chemistry. Assay kits (Wako, Osaka, Japan) were used to measure serum levels of aspartate aminotransferase, ALT, blood urea nitrogen and creatinine, which are biomarkers for hepatic and kidney toxicity. Formalin-fixed liver and kidney samples (#064–00406; Wako) were embedded in Histsec (Merck, Darmstadt, Germany), sliced at 5 μm using a microtome (Leica Microsystems, Wetzlar, Germany) and stained with Carrazzi's hematoxylin and Tissue-Tek eosin solutions (Sakura Finetek USA, Torrance, CA) for histopathological examination. Frozen liver tissues were placed in Tissue-Tek Intermediate cryomolds (#4566; Sakura Finetek USA) filled with precooled Tissue-Tek O. T.C embedding compound (#4583; Sakura Finetek USA) and flash-frozen by immersion in liquid nitrogen. Samples were sliced at 5 μm using a Leica CM1850 (Model 1850-11-1; Leica Biosystems, Wetzlar, Germany) and were air-dried for an hour. The resulting sections were rinsed with distilled water for 30 s and 60% 2-propanol (#03065-35; Nakarai Tesque, Kyoto, Japan) for 60 s. Oil Red O staining stock solution was prepared by dissolving 0.3 g of Oil Red O dye (#154–02072; Wako) in 100 mL of 2-propanol with gentle overnight incubation at 60 °C. Then, 30 mL of stock solution was diluted with 20 mL of distilled water to give a working solution. Samples were stained with this working solution at 37 °C for 15 min, rinsed with 60% 2-propanol and distilled water, and stained with hematoxylin (Gill's Formula) (#H-3401; Vector, Burlingame, CA) solution (25% in PBS) for 2 min at room temperature for histological analysis.

2.7. Statistical analysis

Pharmacological studies were performed with 4–9 mice per treatment group. All data are expressed as means ± SD. $P < 0.05$ was considered to be statistically significant in all cases. Statistical comparisons of results were performed by Dunnett's multiple comparison tests.

3. Results

3.1. Design and physicochemical properties of anti-apoC-III LNA–AON

We first designed AONs targeting apoC-III carrying LNAs (**A301SL**). We placed nine LNAs in the strand, keeping a six natural-nucleotide gap, which is thought to be sufficient for the introduction of RNase H-mediated scission of the mRNA strand (Yamamoto et al., 2012). At the same time, we prepared a corresponding conventional phosphorothioate AON designated **A301S** (Table 1). **A301SL**, **A301S** and 2′-*O*-methoxyethyl RNA-based apoC-III AON, reported previously by Graham et al. (2013), possess the phosphorothioate backbone, but they have different target sequences. As introduction of 2′-*O*-methoxyethyl RNAs into conventional phosphorothioate AONs moderately improves mRNA binding and in vivo antisense potency, **A301S** is speculated to have weaker potential than 2′-*O*-methoxyethyl RNA-based AON. Ideally, the potency and toxicity characteristics of **A301SL** should be compared with those of a corresponding 2′-*O*-methoxyethyl RNA-containing counterpart; however, as we were unable to obtain their phosphoroamidites, we herein utilized **A301S** as a non-LNA control. Note that the sequence, length and composition of AONs have not been fully optimized. A thermal melting study was carried out and T_m values of **A301SL** and **A301S** with their complementary RNA strands were determined. As expected, **A301SL** showed excellent target affinity when compared with conventional phosphorothioate AON (Table 1).

Table 1
Antisense oligonucleotides used in this study.

	Sequence ID	Sequence[a]	T_m (°C)
1	**A301S**	5′-tcttatccagctttattagg-3′	48
2	**A301SL**	5′-TCtTaTCcagcttTaTTaGg-3′	79

[a] Oligonucleotides with LNA (upper case letters) and DNA (lower case letters). All inter nucleotide linkages are phosphorothioated. Melting temperatures (T_m) of 1:1 mixtures of **A301S** and complementary RNA or **A301SL** and complementary RNA.

3.2. Hepatic reduction of apoC-III mRNA expression after systemic administration of LNA–AON

In order to assess the mRNA silencing potency of AONs, we repeatedly administered **A301SL** and **A301S** to C57Bl/6J male mice. After feeding 6-week-old male C57Bl/6J mice a high-fat diet for 2 weeks, mice were subjected to intraperitoneal (i.p.) injection of naked AON at a dosage of 10 and 20 mg/kg/injection five times over 2 weeks. Peripheral blood sampling was performed on day 0 just before the first injection, and on days 8 and 16 post-dose under feed-deprived condition for lipid component analysis and toxicity evaluation. Mice were dissected and their livers were harvested for measurement of gene expression on day 16 post-injection. As shown in Fig. 1, a significant dose-dependent decrease in hepatic apoC-III mRNA levels was only observed in **A301SL**-treated arms. **A301SL** suppressed hepatic apoC-III mRNA expression by ~29% and ~72% on average at a dosage of 10 and 20 mg/kg respectively, while **A301S** failed to achieve any reduction in apoC-III mRNA in the liver, even at the higher dose.

3.3. Serum reduction of apoC-III protein after systemic administration of LNA–AON

Changes in serum apoC-III protein concentration were confirmed by Western blot analysis. Although the quantitative capacity of Western blot analysis is very limited, we found that **A301SL** removed about half of apoC-III protein from sera at a dosage of 20 mg/kg on day 16, while **A301S** showed no significant reductions in apoC-III protein levels, which is consistent with the changes in hepatic apoC-III mRNA expression levels (Fig. 2). Collectively, we

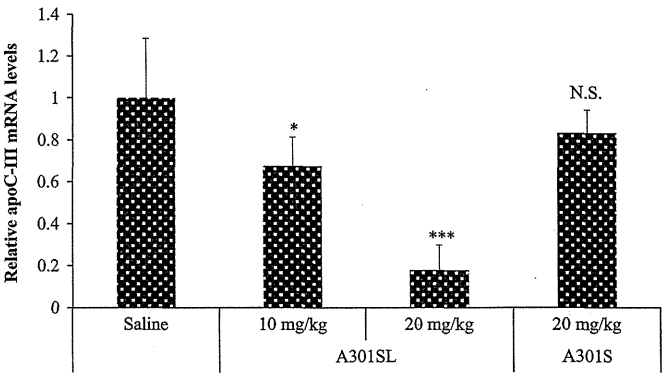

Fig. 1. Hepatic apoC-III mRNA silencing effects of **A301SL** and **A301S**. Western diet-fed mice received intraperitoneal administration of these two AONs at 10 or 20 mg/kg five times over 16 days. Relative hepatic apoC-III mRNA expression levels were determined by means of two-step real-time RT-PCR, and there was a significant reduction in A301SL-treated arms (Dunnett's multiple comparison test, $^{***}P < 0.001$, $^{**}P < 0.01$, $^{*}P < 0.05$, N.S.; not significant). Error bars represent group means+SD.

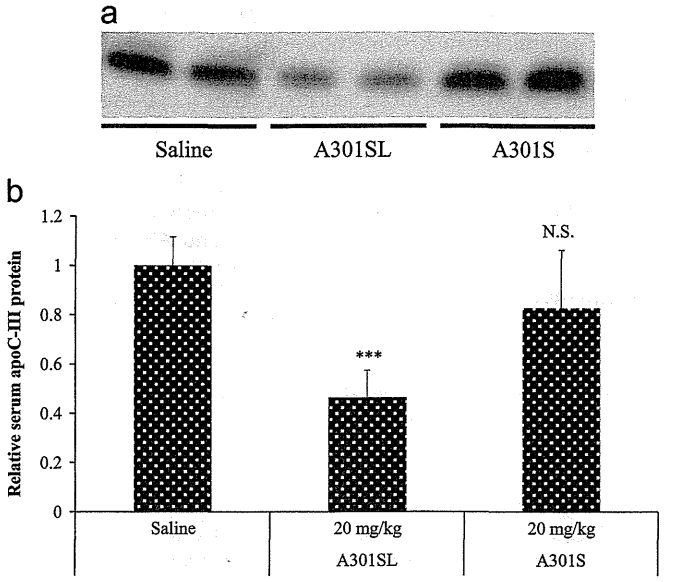

Fig. 2. Effects of **A301SL** and **A301S** on serum apoC-III protein levels. Western diet-fed mice received i.p. administration of these two AONs at 20 mg/kg for five times over 16 days. After completion of dosing, reductions in apoC-III protein level in serum were investigated by Western blotting. (a) Representative images of the membrane, and (b) there was a significant reduction in **A301SL**-treated arms (Dunnett's multiple comparison test, $^{***}P<0.001$, $^{**}P<0.01$, $^{*}P<0.05$, N.S.; not significant). Error bars represent group means ± S.D.

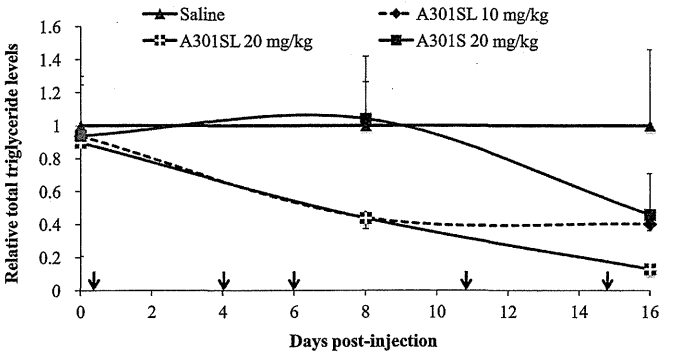

Fig. 3. Effects on serum triglyceride levels over time. Western diet-fed mice received intraperitoneal administration of two AONs, **A301SL** at 10 and 20 mg/kg/injection and **A301S** at 20 mg/kg/injection five times over 16 days. On days 0, 8 and 16, blood samples were collected from tail vein and total triglyceride levels were measured. Dose-dependent reductions were observed in **A301SL** groups, and delayed reductions were seen in the **A301S**-treated arm. Error bars represent group means ± S.D. Arrows indicate the date of administration.

successfully showed that the LNA–AON designed here is a potential inhibitor of apoC-III expression in vivo.

3.4. Serum changes in triglyceride-rich lipoprotein particles concentrations after systemic administration of LNA–AON

To confirm the ability of LNA–AON to modify serum lipids, we assessed the changes in triglyceride contents in fasting peripheral blood collected on days 0, 8 and 16 post-injection. As shown in Fig. 3, **A301SL** was confirmed to reduce serum total triglyceride concentration dose-dependently and more efficiently when compared to **A301S**. Total serum triglyceride levels with a 20 mg/kg/injection of **A301SL** were reduced by ~56% and ~87% over time, as compared to saline-treated controls, whereas **A301S** reduced total serum triglyceride levels by ~54% on day 16. We further conducted HPLC analysis of sera collected on day 8 to determine

Table 2
Serum lipoprotein profiles of hypertriglyceridemic mice on day 8.

	20 mg/kg		
	Saline	A301SL	A301S
Triglyceride [mg/dL]			
Total TG	54.9 ± 13.0	22.1 ± 5.7[b]	51.5 ± 13.1
Chylomicron	0.9 ± 0.5	0.2 ± 0.1[b]	0.5 ± 0.2
Large VLDL	30.3 ± 9.9	5.2 ± 2.3[a]	24.1 ± 7.2
Medium VLDL	10.8 ± 1.7	4.9 ± 1.5[a]	10.4 ± 2.5
Small VLDL	2.9 ± 0.3	2.0 ± 0.5[c]	3.1 ± 0.6
Large LDL	3.4 ± 0.3	2.7 ± 0.7	4.0 ± 0.8
Medium LDL	2.5 ± 0.2	2.3 ± 0.6	3.4 ± 0.8
Small LDL	1.4 ± 0.2	1.3 ± 0.4	1.9 ± 0.4
Very small LDL	1.1 ± 0.2	1.0 ± 0.3	1.3 ± 0.3
Very large HDL	0.28 ± 0.06	0.19 ± 0.05	0.29 ± 0.08
Large HDL	0.26 ± 0.04	0.27 ± 0.11	0.34 ± 0.09
Medium HDL	0.24 ± 0.04	0.49 ± 0.28	0.48 ± 0.18
Small HDL	0.11 ± 0.01	0.59 ± 0.40[c]	0.48 ± 0.23
Very small HDL	0.74 ± 0.09	1.17 ± 0.43	1.13 ± 0.21
Cholesterol [mg/dL]			
TC	133.4 ± 15.6	109.5 ± 11.7*	125.1 ± 14.9
Chylomicron	0.13 ± 0.05	0.04 ± 0.02[a]	0.07 ± 0.02[b]
Large VLDL	6.3 ± 1.8	1.3 ± 0.5[a]	3.9 ± 0.7[a]
Medium VLDL	4.7 ± 0.9	2.6 ± 0.6[a]	2.9 ± 0.4[a]
Small VLDL	3.0 ± 0.5	2.7 ± 0.8	2.4 ± 0.4
Large LDL	5.0 ± 0.6	5.0 ± 1.4	4.8 ± 0.7
Medium LDL	4.9 ± 0.6	5.2 ± 1.6	5.9 ± 0.8
Small LDL	3.4 ± 0.4	3.6 ± 1.1	4.4 ± 0.7
Very small LDL	6.1 ± 2.3	5.6 ± 2.0	11.7 ± 3.8[c]
Very large HDL	7.5 ± 2.3	7.2 ± 2.3	9.1 ± 1.7
Large HDL	32.1 ± 5.2	27.9 ± 3.3	29.4 ± 3.3
Medium HDL	35.3 ± 3.4	28.6 ± 1.1[b]	29.9 ± 3.2[c]
Small HDL	15.7 ± 1.0	12.1 ± 0.2[a]	12.5 ± 1.7[b]
Very small HDL	9.1 ± 0.8	7.6 ± 0.5[c]	8.0 ± 1.0

TG; triglyceride, TC; total cholesterol. Data are means ± S.D.
[a] $P<0.001$ vs. saline group.
[b] $P<0.01$ vs. saline group.
[c] $P<0.05$ vs. saline group.

the precise serum lipid profile. HPLC analysis revealed that **A301SL** markedly reduced VLDL-triglycerides, and larger VLDL-triglycerides were preferentially removed (Table 2). Moreover, substantial reductions in VLDL- and HDL-cholesterol were also observed in the **A301SL**-treated arm, and a much milder but similar trend was seen in the **A301S**-treated arm. These trends were particularly evident on day 16 (Fig. 4), and are consistent with the slight but not significant reductions in hepatic apoC-III mRNA and serum apoC-III protein levels, as shown in Figs. 1 and 2 on day 16.

3.5. Histopathological analysis of murine liver and kidneys

Pharmacological and toxicological characteristics of **A301SL** upon dosing were estimated by histopathological analysis. While all individuals in the saline group showed fat accumulation in the liver, induced by the Western diet, no such findings were observed in the **A301S**- and **A301SL**-treated arms (Fig. 5 and Table 3). We further visualized and compared fat drops in the livers by direct lipid staining with Oil Red O. As shown in Fig. 5, LNA–AON markedly reduced hepatic fat accumulation. Histopathologically, no severe cellular damage was noted, even at the highest doses in the centrilobular and perilobular hepatocytes, which were frequently seen after toxicological insult. On the other hand, moderate granulomas and granular degeneration were observed in the liver. Serum chemistry profiles showed slight increases in serum

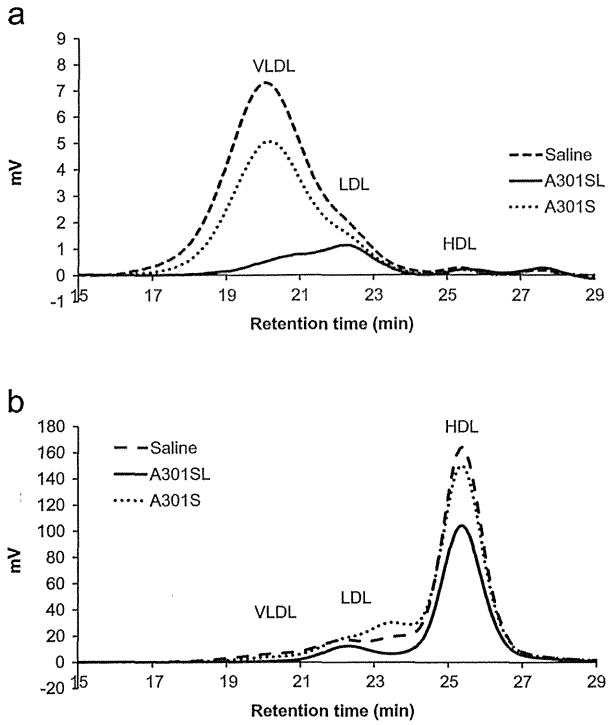

Fig. 4. Representative HPLC lipoprotein profiles of western diet-fed C57BL/6J mice received intraperitoneal administration of saline (dashed line), **A301SL** (solid line) at 20 mg/kg/injection or **A301S** (dotted line) at 20 mg/kg/injection five times over 16 days. Five saline-, **A301SL**- and **A301S**-treated mice were analyzed and the data from one representative individual mouse were presented. Corresponding (a) triglyceride and (b) cholesterol profiles were obtained from one identical mouse in each arm.

transaminases and slight decreases in blood urea nitrogen (Table 4). Elevations in transaminases may be due to the granular degeneration of hepatocytes. There were no significant changes in serum creatinine levels in each group.

4. Discussion

We have scarcely obtained selective inhibitors of apoC-III, which is thought to be a potential drug for the treatment of dyslipidemia, diabetes and cardiovascular diseases, as well as a useful tool for elucidation of the physiological roles of apoC-III. To develop a selective inhibitor of apoC-III, we designed an LNA-based 20-mer phosphorothioated AON (**A301SL**), in which LNAs are expected to greatly help with the target binding for the usage in vivo. As expected, **A301SL** achieved efficient dose-dependent reductions in hepatic apoC-III mRNA and decreased serum apoC-III protein concentration, which could be associated with the observation of efficient dose-dependent reductions in serum triglyceride concentration and attenuation of fat in the liver. *One limitation is that serum change of apoC-III protein was here confirmed by semiquantitative Western blot analysis.* For further study, we moved onto a precise lipoprotein profiling analysis of sera using HPLC methodology. Through this analysis, we found that serum reductions in triglycerides and cholesterol levels were largely a result of decreases in VLDL-triglycerides and VLDL-cholesterol from sera. It is also noteworthy that larger-sized VLDL was more susceptible to removal from blood, resulting in a shift of particle size distribution to smaller diameters (Table 2 and Fig. 4). Generally, large triglyceride-rich VLDL-1 are preferentially converted into atherogenic small, dense LDL, through a process mediated principally by cholesteryl ester transfer protein, lipoprotein lipase and hepatic lipase (Millar and Packard, 1998). Lipoprotein lipase activity is known to be modified by apoC-III protein and lipoprotein lipase preferentially hydrolyzes larger triglycerides-rich VLDL subfractions than smaller particles (Fisher et al., 1995). Thus, preferential removal of triglycerides from larger VLDL particles observed here can be explained as a result of derepression of lipoprotein lipase activity *via* successful silencing of apoC-III with LNA–AON. Combined with previous observations that, among triglycerides-rich lipoprotein subfractions in combined hyperlipidemia patients such as type IIb, VLDL-1 has the highest potential to induce accumulation of triglycerides and cholesterol in macrophages and foam cell formation (Milosavljevic et al., 2001), selective apoC-III inhibitors would possibly show anti-atherogenic phenotype.

Both apoC-III-null subjects and apoC-III-deficient mice generally possess reduced plasma total cholesterol levels, as well as total triglycerides, when compared to those of normal controls (Gerritsen et al., 2005; Jong et al., 2001; Pollin et al., 2008; Takahashi et al., 2003). We also observed a 33% reduction in total cholesterol levels along with apoC-III attenuation by the LNA–AON. This decrease in plasma cholesterol levels was reflected in both apolipoprotein B-containing and HDL fractions (Table 2 and Fig. 4). However, the mechanistic background for the reduction of plasma cholesterol upon apoC-III attenuation is controversial. A previous study showed that apoC-III deficiency in apolipoprotein E-knockout mice accelerated the kinetics of uptake of cholesterol ester, which is related to the function of hepatic lipase (Jong et al., 2001). In addition, hepatic lipase transgenic rabbits and hepatic lipase transgenic and adenovirus-transduced mice were reported to reduce plasma triglycerides and apolipoprotein B-containing lipoprotein cholesterols as well as HDL cholesterol (Applebaum-Bowden et al., 1996; Busch et al., 1994; Dichek et al., 1998; Fan et al., 1994). As our findings are in line with these previous observations, we speculate that activation of hepatic lipase resulting from apoC-III attenuation by the LNA–AON caused a reduction in plasma cholesterol levels. In contrast, Old Order Amish individuals with an *APOC3*-null mutation have higher plasma HDL cholesterol concentrations, as well as lower levels of triglycerides and non-HDL cholesterol than those of normal subjects (Pollin et al., 2008). In addition, knockout effects of apoC-III on plasma cholesterol levels also vary between genetic backgrounds of mice and experimental conditions (Jong et al., 2001; Takahashi et al., 2003). There are only a small number of reports focusing on the relationship between cholesterol metabolism and apoC-III (Kinnunen and Ehnholm, 1976). To determine the true effects of apoC-III modulation on cholesterol metabolism, further experimental data is necessary.

The toxicological characteristics of **A301SL** and **A301S** were estimated based on serum biochemistry characteristics and histopathological analysis. As phosphorothioated AONs accumulate mainly in the kidney and liver, hepatotoxicity and/or nephrotoxicity are primary concerns. Our experiments found only moderate hepatotoxicity for **A301SL** and **A301S,** as shown in the moderate increases in liver transaminases and decreases in blood urea nitrogen, while no significant changes in serum creatinine levels were noted. Histopathological observations supported these data (Fig. 5, Tables 3 and 4). Similar hepatotoxicity attributable to LNA-modified phosphorothioated AONs, which was avoidable by substituting 2′,4′-BNA^{NC} chemistry for LNA, has been reported (Prakash et al., 2010; Yamamoto et al., 2012). Dose-related hepatotoxicity could be tolerable based on the systemic AON recently approved by the US Food and Drug Administration (FDA) named "Kynamro", which also shows serum elevation of transaminases, specifically alanine aminotransferase (ALT) (http://www.kynamro.com/). However, it is necessary to determine how AONs trigger toxicity in order to resolve this issue (Levin, 1999). Therefore, we further conducted Oil Red O staining of liver samples. The results